

N 73-28918

NASA TECHNICAL
MEMORANDUM



NASA TM X-2857

NASA TM X-2857

CASE FILE
COPY

PERFORMANCE OF
AN ANNULAR COMBUSTOR DESIGNED
FOR A LOW-COST TURBOJET ENGINE

by James S. Fear

*Lewis Research Center
Cleveland, Ohio 44135*

1. Report No. NASA TM X-2857		2. Government Accession No.		3. Recipient's Catalog No.	
4. Title and Subtitle PERFORMANCE OF AN ANNULAR COMBUSTOR DESIGNED FOR A LOW-COST TURBOJET ENGINE				5. Report Date August 1973	
				6. Performing Organization Code	
7. Author(s) James S. Fear				8. Performing Organization Report No. E-7424	
9. Performing Organization Name and Address Lewis Research Center National Aeronautics and Space Administration Cleveland, Ohio 44135				10. Work Unit No. 501-24	
				11. Contract or Grant No.	
12. Sponsoring Agency Name and Address National Aeronautics and Space Administration Washington, D.C. 20546				13. Type of Report and Period Covered Technical Memorandum	
				14. Sponsoring Agency Code	
15. Supplementary Notes					
16. Abstract <p>Performance tests were conducted on a combustor designed for use in a low-cost turbojet engine. Low-cost features included the use of very inexpensive simplex fuel nozzles and combustor liners of perforated sheet material. Combustion efficiencies at the altitude-cruise and sea-level design points were approximately 94 and 96 percent, respectively. The combustor isothermal total-pressure loss was 8.8 percent at the altitude-cruise-condition diffuser-inlet Mach number of 0.335. The combustor-exit temperature pattern factor was less than 0.3 at the altitude-cruise, sea-level-cruise, and sea-level-static design conditions. The combustor-exit average radial temperature profiles at all conditions were in very good agreement with the design profile. The intense mixing required because of the very high combustor heat-release rate had an adverse effect on ignition capability at altitude windmilling design conditions.</p>					
17. Key Words (Suggested by Author(s)) Low-cost combustor Small turbojet engine			18. Distribution Statement Unclassified - unlimited		
19. Security Classif. (of this report) Unclassified		20. Security Classif. (of this page) Unclassified		22. Price* \$3.00	
				21. No. of Pages 42	

Page Intentionally Left Blank

PERFORMANCE OF AN ANNULAR COMBUSTOR DESIGNED FOR A LOW-COST TURBOJET ENGINE

by James S. Fear

Lewis Research Center

SUMMARY

Performance tests were conducted on a combustor designed for use in a low-cost turbojet engine. Inexpensive simplex nozzles were used for fuel atomization. Film-cooled combustor liners were made of perforated sheet. The inner combustor housing wall was eliminated. The combustor was designed for inlet-air conditions of 439 K (331° F) and 28.1 N/cm² (40.8 psia) and an exit temperature of 1089 K (1500° F), corresponding to Mach 0.80 cruise at an altitude of 6096 meters (20 000 ft); and for inlet-air conditions of 492 K (426° F) and 54.0 N/cm² (78.3 psia) and an exit temperature of 1119 K (1555° F), corresponding to Mach 0.80 cruise at sea level. At the sea-level-static design point, the inlet conditions were 455 K (359° F) and 38.5 N/cm² (55.8 psia), and the design exit temperature was 1089 K (1500° F).

Combustion efficiencies at the altitude-cruise and sea-level-cruise design points were approximately 94 and 96 percent, respectively. The combustor isothermal total-pressure loss was 8.8 percent at the altitude-cruise-condition diffuser-inlet Mach number of 0.335 and 9.8 percent at the sea-level-cruise condition diffuser-inlet Mach number of 0.355. Combustor-exit temperature pattern factors were less than 0.3 at the three design points described above. The combustor-exit average radial temperature profiles at all design conditions were in good agreement with design profiles. Because of the unusually high combustor heat-release rate, intense mixing was required to obtain good combustor-exit temperature pattern factors. This requirement caused combustor total-pressure losses to be somewhat higher than those usually reported for combustors with less severe heat-release rates, and it was detrimental to the ability to ignite at altitude windmilling conditions.

INTRODUCTION

This test program was conducted to develop low-cost combustor technology for use in small turbojet engines.

As part of the gas-turbine technology program at the NASA Lewis Research Center, studies have been made of the feasibility of reducing the total manufactured cost of small turbojet or turbofan engines to one-quarter or less of the cost of current engines of similar thrust level (ref. 1). This cost reduction would allow turbojet and turbofan engines to compete on a cost basis with reciprocating or turboprop engines for light aircraft use. As a result of studies of aircraft flight requirements, engine cycle characteristics, and design cost-reduction potential, both a turbojet engine and a turbofan engine were selected to serve as focuses for the technology program (refs. 1 to 3). The turbojet engine was designed with a single-stage turbine and a four-stage axial compressor with a 4:1 compression ratio. A combustor suitable for use in this engine was designed and tested, and performance results are presented in reference 4.

Because of its potential for low production cost, compactness, and light weight, the low-cost turbojet engine is attractive for expendable use in missiles or drones, where it can provide greater range and payload capacity than can be achieved by a rocket engine. Typical requirements for such an engine are discussed in reference 5. At a design flight Mach number of 0.8 at 6096 meters (20 000 ft) altitude, a thrust of 1557 newtons (350 lbf) is required. The sea-level static thrust is 2891 newtons (650 lbf). The weight limit is 45.4 kilograms (100 lbm), the diameter limit is 0.31 meter (12 in.), and the specific fuel consumption must be below 0.18 kg/hr/newton (1.8 lbm/hr/lbf). Windmilling startup under ram conditions at altitude is required, as well as sea-level startup under ram conditions or under static conditions by compressed air impingement on the turbine rotor.

A turbojet engine intended as a test bed for low-cost technology was designed to meet these requirements while utilizing the low-cost fabrication techniques described in reference 4. This report describes the design of the combustor for the selected engine and presents the results of combustor performance tests.

SCOPE OF INVESTIGATION

~~A combustor was designed and developed to meet the performance requirement of~~
the low-cost turbojet engine and, at the same time, to utilize cost-reducing design innovations. Some of these innovations are:

- (1) The use of a plain perforated-sheet liner for film cooling instead of scoops, louvers, and so forth
- (2) The elimination of an inner combustor housing wall and the use of the engine rotating shaft instead
- (3) The elimination of costly duplex or variable-area fuel nozzles and the use of very inexpensive simplex fuel nozzles

Performance data were obtained at four design points (table I) - sea-level static (100-percent engine speed), sea-level idle, cruise at a flight Mach number of 0.8 at an altitude of 6096 meters (20 000 ft), and cruise at a flight Mach number of 0.8 at sea level.

ASTM A-1 fuel at ambient temperature was used in all tests. Performance data included combustion efficiency, combustor total-pressure loss, combustor-exit temperature profiles, windmilling ignition data, blowout data, smoke formation and exhaust emissions, and durability.

The test facility and instrumentation used are described in appendixes A and B, respectively.

DESCRIPTION OF COMBUSTOR

Type of Combustor

The combustor tested (fig. 1 and table II) was designed using the annular one-sided-air-entry approach described in references 6 and 7 and using experience gained in testing the combustor described in reference 4. In this approach, most of the combustion air enters through the outer combustor liner, with lesser amounts going through the combustor snout and firewall to aid in fuel atomization and going to the inner combustor liner for cooling purposes only. Figure 2 shows a typical distribution of combustion air in a one-sided-air-entry combustor. No critical air splits between inner and outer annuli are required to maintain recirculation and dilution zones in the combustor. Thus, effects of radial distortions in compressor flow are minimized, and a suitable combustor-exit temperature profile is achieved even at off-design conditions.

It has been found that small combustors do not operate as efficiently as larger combustors (ref. 8). This effect has been correlated as a function of the combustor hydraulic radius. The hydraulic radius of the one-sided-air-entry combustor can be maximized for a given combustor cross-sectional area by use of the space close to the rotating shaft. Use of this space is possible because only a narrow passage is required for the small amount of cooling air for the inner combustor liner. The hydraulic radius has been further increased, and weight and cost reduced, by the elimination of the inner combustor housing wall. The combustor-inner-liner cooling air flows between the liner and the rotating shaft, which functions as the inner housing wall.

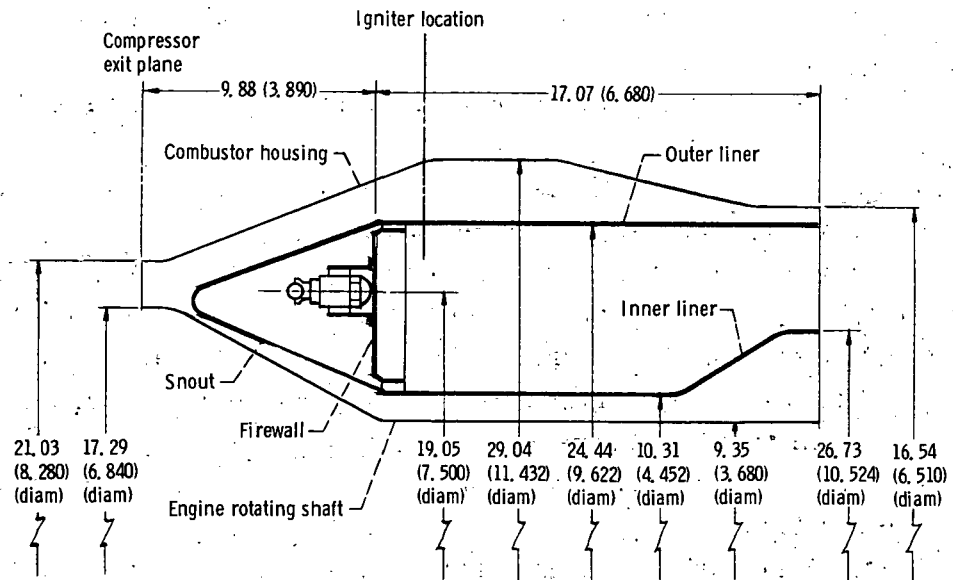


Figure 1. - Dimensions of low-cost combustor. Dimensions are in centimeters (in.).

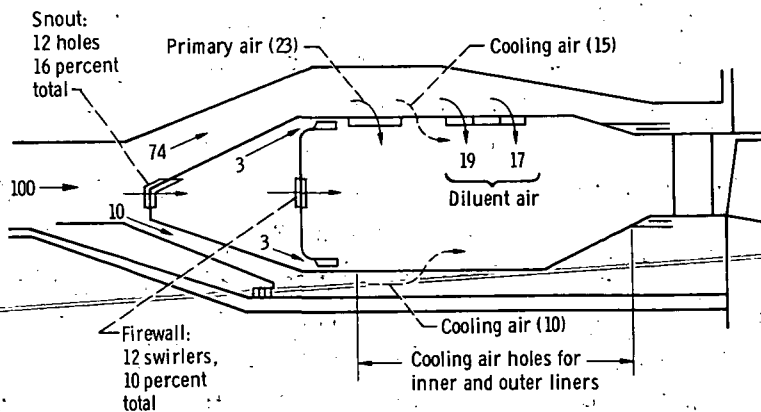
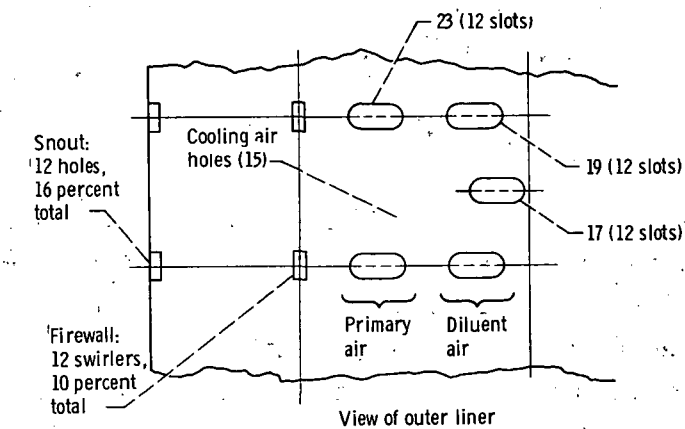


Figure 2. - Typical combustion air distribution in annular one-sided-air-entry-type combustor. Numbers indicate percentages of total airflow rate.

Combustor Liner Design

The use of perforated-sheet combustor liners is appealing from a cost standpoint. The effectiveness of film cooling through the use of circular holes has been investigated and is reported in reference 9. In using perforated-sheet film cooling, two facts must be considered:

(1) The cooling jet does not spread laterally to any appreciable extent.

(2) If the jet has a high velocity, it will penetrate into the main air stream and will not provide a high cooling effectiveness.

The lateral spread limitation can be overcome by proper orientation of the cooling-hole pattern (fig. 3). It is necessary only that the hole pattern repeat by the time the jet is dissipated in the axial direction. The cooling jets function most efficiently when the ratio of the momentum of the cooling stream to that of the main airstream is of the order of 0.5; however, fairly good efficiencies can be maintained with momentum ratios from approximately 0.2 to 0.8. This means that the perforated-sheet method of film cooling will accommodate a wide range of diffuser efficiencies without severe deterioration of film-cooling effectiveness.

For good cooling effectiveness, it is generally advantageous to have many holes of smaller diameter, rather than fewer holes of larger diameter, for a given total open area. The particular hole pattern chosen was a compromise. The pattern shown in figure 3 is a relatively coarse one, and its selection was dictated by the consideration that fine hole patterns are difficult to manufacture in materials typically used in combustor liners. Preliminary tests showed this pattern to be satisfactory (ref. 10), and this was confirmed in subsequent testing of the combustor described in reference 4 and in the combustor described in this report.

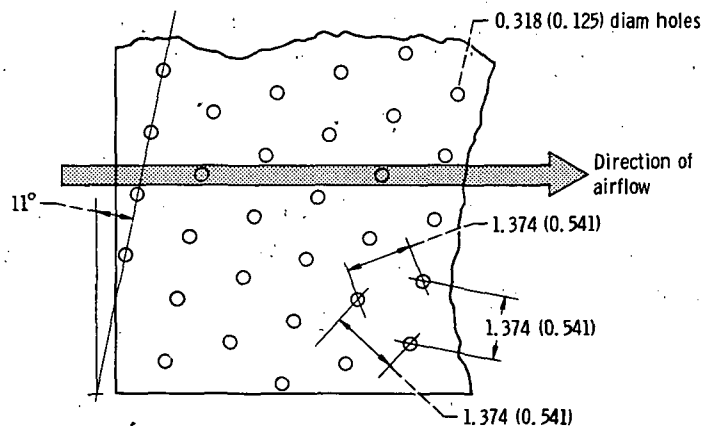


Figure 3. - Orientation of perforated sheet liner for optimum film cooling.
Dimensions are in centimeters (in.).

The primary-zone and dilution-zone air-entry-hole patterns were established on the basis of jet penetration theory and previous combustor design experience. Two sets of diluent holes are used - one for deep penetration to the inner combustor liner, and the second for shallow penetration into the region near the outer liner. The pattern used on the final combustor liner design is shown in figure 4, and a summary of final design combustor dimensions is given in table II.

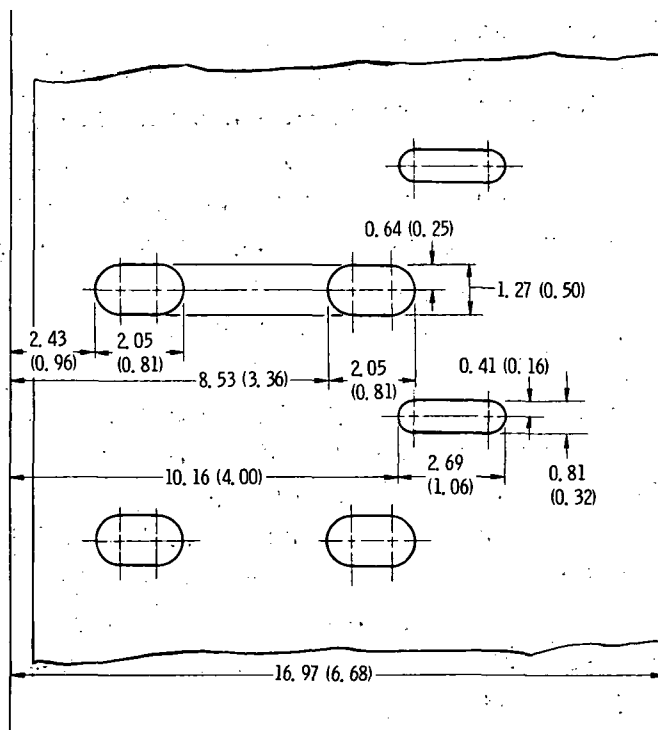


Figure 4. - Primary-zone and diluent-zone air-entry hole pattern for final combustor design. Dimensions are in centimeters (in.).

Ignition

Two surface-discharge-type igniters, 10^0 above the horizontal centerline of the combustor on either side, were used. The ignition exciters were supplied with 24-volt dc electrical power and had an energy level of 12 joules.

Fuel Atomization

Fuel was introduced at 12 circumferential locations through Monarch simplex nozzles of the type customarily used in home oil furnaces. The nozzles were as shown in

figure 5, with a flow rate of $0.04 \text{ m}^3/\text{hr}$ (10.5 gal/hr) for each nozzle, at a nozzle pressure drop of 69 N/cm^2 (100 psi). These nozzles were set in six-bladed swirlers in the combustor firewall (fig. 6) and were manifolded inside the combustor snout, with a single fuel tube supplying the fuel manifold.



C-71-1222

Figure 5. - Monarch simplex fuel nozzle.

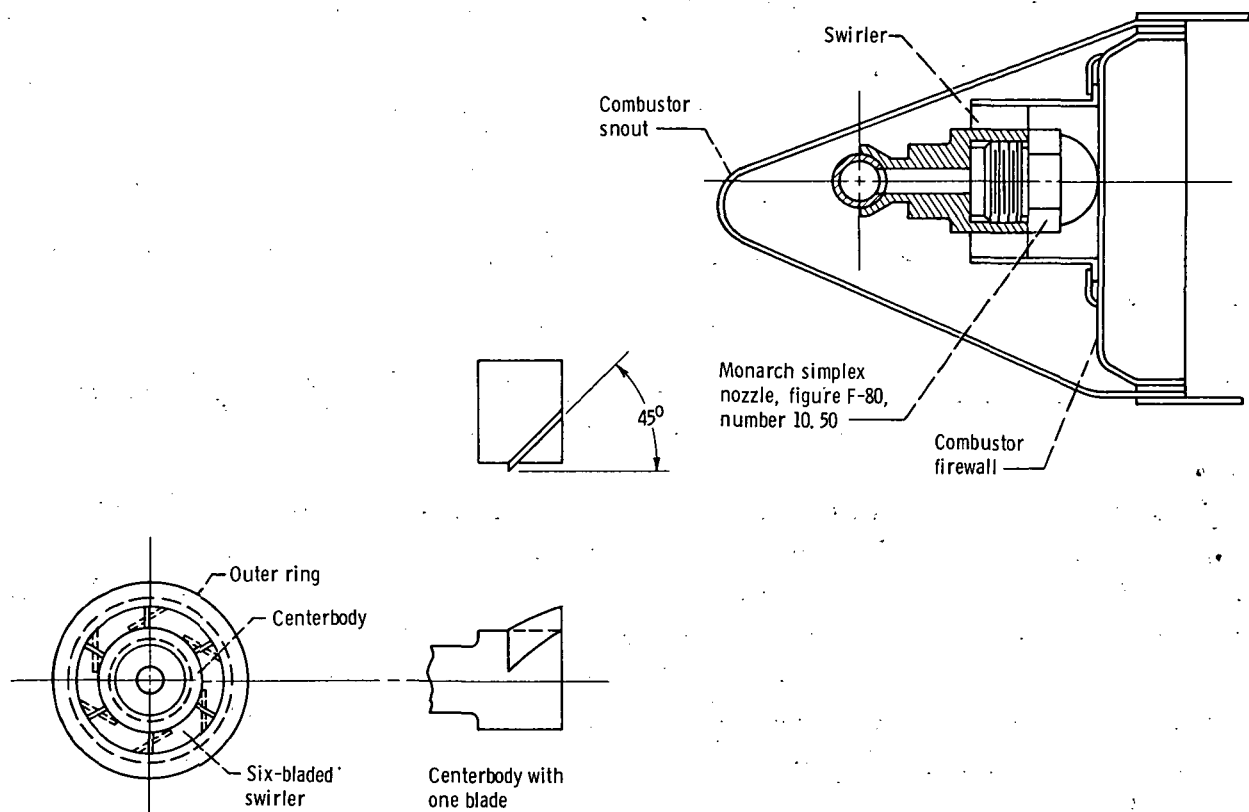


Figure 6. - Fuel nozzle and swirler arrangement.

CALCULATIONS

Combustion Efficiency

Combustion efficiency was calculated by dividing the measured temperature rise across the combustor by the theoretical temperature rise. The diffuser-inlet temperature was taken as the arithmetic average of six thermocouple readings. The combustor-exit temperature was taken as the arithmetic average of 80 thermocouple readings. Since the thermocouple rakes were not cooled and the surrounding combustor parts were at essentially the same temperature as the thermocouples, no radiation correction was required; and the indicated readings of the thermocouples were taken as true values.

Reference Velocity

Combustor reference velocity was calculated from the total airflow rate, the maximum cross-sectional area of the combustor housing, and the air density based on the total pressure and total temperature at the diffuser inlet.

Total-Pressure Loss

The combustor total-pressure loss includes diffuser total-pressure losses and is defined as

$$\frac{\Delta P}{P} = \frac{(\text{Average diffuser-inlet total pressure}) - (\text{Average combustor-exit total pressure})}{\text{Average diffuser-inlet total pressure}}$$

The total-pressure loss was calculated from the arithmetic averages of 8 total pressures measured at the diffuser inlet and of 10 total pressures measured at the combustor exit. The number of readings was limited by the number of pressure transducers available for data recording. Manometer tubes, giving 24 pressure readings at the diffuser inlet and 30 at the combustor exit, were used periodically as a check. The diffuser-inlet Mach numbers used to correlate total-pressure loss were calculated from the static pressure, total temperature, and cross-sectional area measured at the diffuser inlet and from the total combustor airflow.

Exit Temperature Profile Parameters

Three parameters often used in evaluating the quality of combustor-exit temperature profiles are considered. The first is the exit temperature pattern factor δ , defined as

$$\delta = \frac{T_{\text{exit,max}} - T_{\text{exit,av}}}{T_{\text{exit,av}} - T_{\text{inlet,av}}}$$

where $T_{\text{exit,max}} - T_{\text{exit,av}}$ is the maximum temperature occurring anywhere in the combustor-exit plane minus the average combustor-exit temperature. The term $T_{\text{exit,av}} - T_{\text{inlet,av}}$ is used in all three parameters and is the average temperature rise across the combustor. This parameter considers the maximum positive difference between an individual temperature and the average temperature, but it does not take into account the design radial temperature profile of the combustor. A temperature which is higher than the average combustor-exit temperature may be only slightly above the desired temperature at the midspan of a turbine blade, while the same temperature would be excessively high at the blade hub. Two parameters which taken the design profile into account are

$$\delta_{\text{stator}} = \frac{(T_{r,\text{exit,local}} - T_{r,\text{exit,design}})_{\text{max}}}{T_{\text{exit,av}} - T_{\text{inlet,av}}}$$

and

$$\delta_{\text{rotor}} = \frac{(T_{r,\text{exit,av}} - T_{r,\text{exit,design}})_{\text{max}}}{T_{\text{exit,av}} - T_{\text{inlet,av}}}$$

where $(T_{r,\text{exit,local}} - T_{r,\text{exit,design}})_{\text{max}}$ for δ_{stator} is the largest positive temperature difference between the highest local temperature at any given radius and the design temperature for that radius; and where $(T_{r,\text{exit,av}} - T_{r,\text{exit,design}})_{\text{max}}$ for δ_{rotor} is the largest positive or negative temperature difference between the average radial temperature at any given radius and the design temperature for that radius. In the case of δ_{stator} the maximum excess in local temperature is considered because a stator blade continuously "sees" this temperature; a rotor blade periodically passes through the region of high temperature, so that a point on a given radius of the rotor blade "sees" the average temperature for that radius. Thus the maximum difference in aver-

age temperature is used in calculating δ_{rotor} . Only a positive difference from the design temperature is considered in the calculation of δ_{stator} because a temperature lower than the design temperature is not detrimental to the stator blade. Both positive and negative differences from design temperature are considered in the calculation of δ_{rotor} because a temperature lower than the design temperature, while not causing harm to the rotor blade, results in a deficiency in the work extracted from the gas stream by the turbine compared with that extracted with proper thermal loading of the turbine.

Heat-Release Rate

The combustor heat-release rate HRR is calculated as

$$\text{HRR} = \frac{(\text{LHV})(\dot{W}_f)(\eta_c)}{(\text{VOL})(P)}$$

expressed as joules/hr-cm³-atm (Btu/hr-ft³-atm), where LHV is the lower heating value of the fuel in joules/kg (Btu/lbm), \dot{W}_f is the fuel flow rate in kg/hr (lbm/hr), η_c is combustion efficiency, VOL is combustor liner volume in cm³ (ft³), and P is combustor inlet total pressure at atmospheres.

Emission Index

Exhaust emissions samples were obtained and analyzed in accordance with SAE Aerospace Recommended Practice ARP 1256 (ref. 11). The equipment used is described in reference 12.

The emission index is defined as the ratio of the number of grams of pollutant formed divided by the number of kilograms of fuel consumed. The amount of pollutant formed can be expressed as

$$\frac{(\text{MW})_P}{(\text{MW})_E} \times \dot{m} \times \text{ppm}$$

where $(\text{MW})_P$ is the molecular weight of the pollutant; $(\text{MW})_E$ the molecular weight of the exhaust products; \dot{m} the total mass flow rate through the combustor, composed of the sum of the air and the fuel flows; and ppm is the concentration of the pollutant in parts per million. Dividing this expression by kilograms of fuel and simplifying gives

the emission index

$$EI = \frac{(MW)_P}{29} \times 10^{-3} \times \frac{1 + \frac{f}{a}}{\frac{f}{a}} \times \text{ppm}$$

where f/a is the fuel-air ratio. Values used for the molecular weight of the pollutant are 30 for nitric oxide, 28 for carbon monoxide, and 14 for hydrocarbons. The assumed molecular weight of the exhaust products is 29.

Smoke Number

The exhaust gas sample was obtained and analyzed in accordance with SAE Aerospace Recommended Practice ARP 1179 (ref. 11). Smoke number measurements were obtained by drawing a metered volume of exhaust gas through a filter of Whatman Number 4 filter paper, which collected all smoke particles suspended in the gas.

The absolute reflectivity of the smoke traces was read with a Welch Densichron. The instrument was calibrated with gray-scale tiles supplied by the manufacturer. All sample traces were read over a gray background with an absolute reflectivity of 31.5 percent. The absolute reflectivity of the clean Whatman Number 4 filter paper read over the gray background was 77.5 percent.

The density of the smoke sample was expressed as a smoke number, which is defined by the following equation:

$$\text{Smoke number} = 100 \left(1 - \frac{R_s}{R_w} \right)$$

where R_s is percent absolute reflectivity of sample and R_w is percent absolute reflectivity of clean filter paper (77.5 percent).

Units

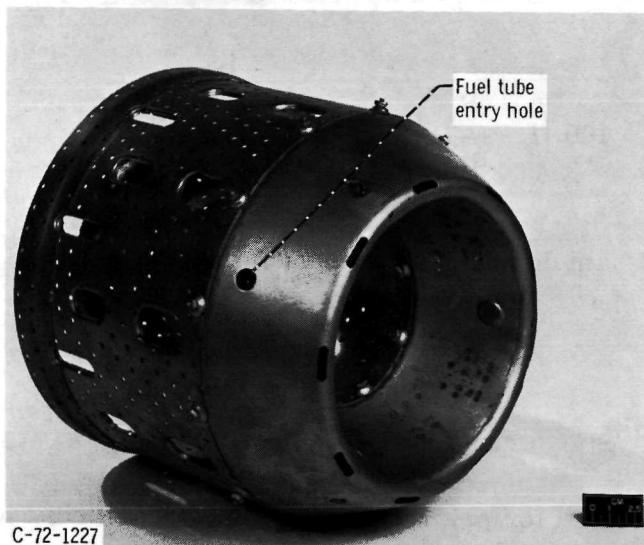
The U.S. customary system of units was used for primary measurements and calculations. Conversion to SI units (Système International d'Unités) is done for reporting purposes only. In making the conversion, consideration is given to implied accuracy and may result in rounding off the value expressed in SI units.

RESULTS AND DISCUSSION

Combustor Development

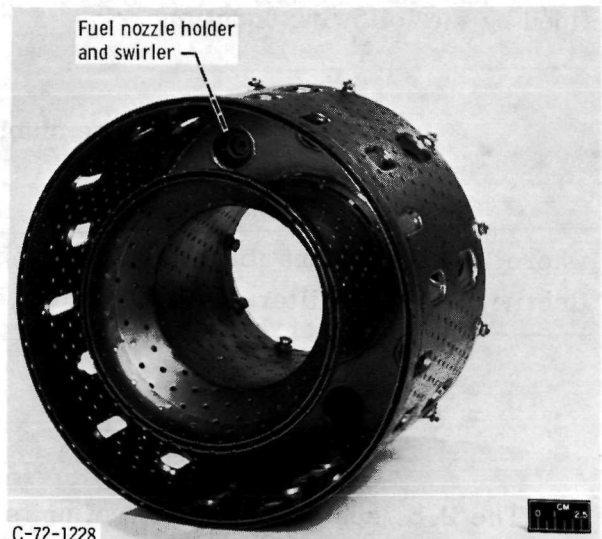
The first model of the low-cost combustor is shown in figure 7. This model was directly scaled from the simplex nozzle combustor described in reference 4. In general, linear dimensions were scaled to 72 percent as compared with the earlier combustor. Thus, the cross-sectional area was now 52 percent and the combustor volume 37 percent of the original values. The number of fuel nozzles was reduced from 12 to nine so that the arc distance between nozzles was approximately the same as before. The number of air-entry holes in the primary zone and in the two diluent hole rows was reduced from 12 to nine to correspond with the fuel nozzle reduction. Their areas were chosen so that the total hole area was scaled correctly, although the individual hole area was not. The air-entry holes were of the plunged type. The component parts of this model were fastened together with screws to facilitate modifications during development.

Early test results were satisfactory with regard to combustion efficiency and total-pressure loss; however, combustor-exit temperature pattern factors were unsatisfactory. Numerous variations were made in the sizes of the primary-zone and diluent-zone air-entry holes to promote good mixing and uniform combustor-exit temperature distribution. In a number of cases, good pattern factors were obtained at moderate combustor heat-release rates; but as the fuel-flow rate was increased to the design value, a point would be reached at which an increase in the pattern factor to an unacceptable level would



C-72-1227

(a) Upstream view.



C-72-1228

(b) Downstream view.

Figure 7. - First model of low-cost combustor.

occur. The use of larger-capacity fuel nozzles appeared to delay the increase in pattern factor until a higher fuel-flow rate was reached. This apparent delay suggests the possibility that, at high fuel-nozzle pressure-drop levels, the momentum of the fuel caused some of it to burn further downstream in the combustor than desired, precluding proper mixing with diluent air before it left the combustor.

A combustor was tested in which the number of fuel nozzles was increased from nine to 12 and the number of primary-zone and diluent-zone air-entry holes was changed to 12 and they were sized accordingly. This change caused the arc distance between the fuel injection points to decrease from 6.65 centimeters (2.62 in.) to 4.98 centimeters (1.96 in.) and resulted in an improvement in pattern factor. However, pattern factors were still too high at the design fuel-flow rate. Two modifications were made to introduce more air into the primary zone and to improve mixing. The first was an increase in the size of the combustor snout air-entry holes. The second was a decrease in the sizes of the primary-zone and diluent-zone air-entry holes in the combustor liner. The combined effect of these modifications was to cause a leaner fuel-air mixture in the primary zone with better mixing. Pattern factors were improved significantly, while total-pressure loss increased slightly and combustor blowout limits became somewhat poorer. The final model of the low-cost combustor, in which the combustor liner holes are flush rather than plunged, is shown in figure 8.

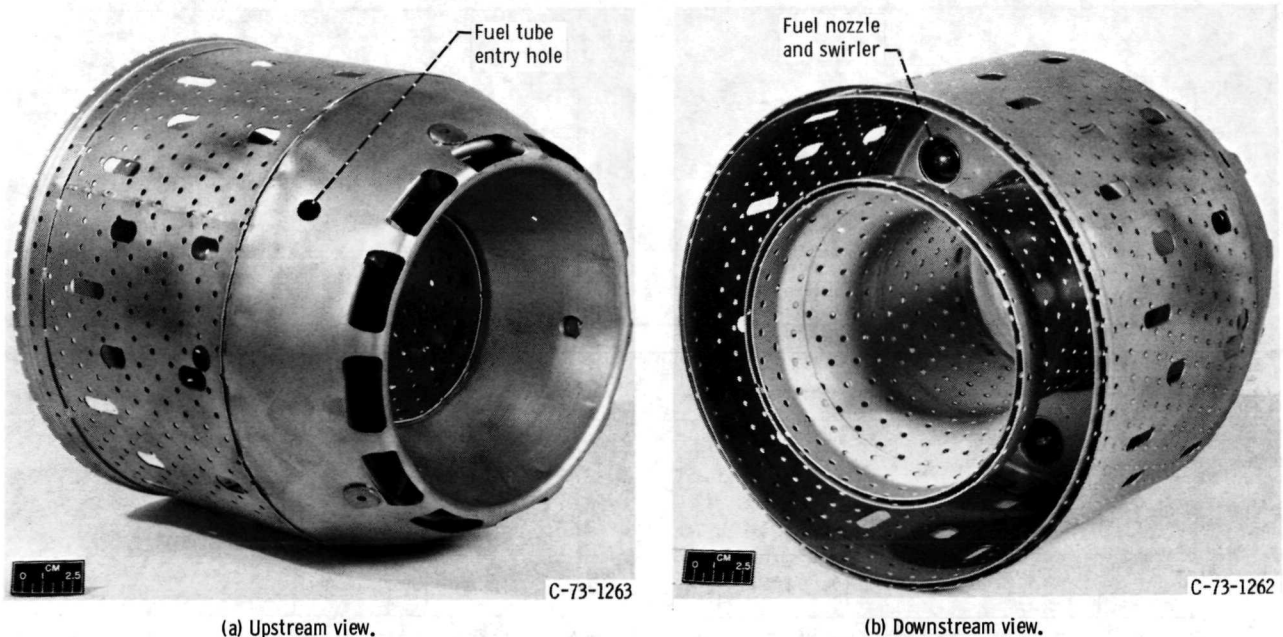


Figure 8. - Final model of low-cost combustor.

Performance Tests

Performance tests of the final combustor design (fig. 1 and table II) were conducted at the nominal test conditions listed in table I. The results of these tests are presented in table III and in the following paragraphs.

Combustion efficiency. - Combustion efficiency data for the low-cost combustor are presented in figure 9. Figure 9(a) shows that the combustion efficiency at the altitude-cruise design point is approximately 94 percent. At the sea-level-cruise point (fig. 9(b)), increased combustor-inlet pressure and temperature cause the combustion efficiency to increase to approximately 96 percent. These efficiencies are adequate because of the short mission times for which the engine will be required to operate. At both cruise design points, the difference between the total amount of fuel to be carried and that needed at a good combustion efficiency, such as 98 percent, is approximately 1.8 kilograms (4 lbf) for a mission duration of 15 minutes. This is not a significant weight penalty, and the specific fuel consumption should be well below the generous limit of 0.18 kg/hr/newton (1.8 lbf/hr/lbf).

Combustion efficiency at the sea-level-static condition (100-percent engine speed) is shown in figure 9(c) to be approximately 96 percent at the design point. This condition would apply to a takeoff at sea level after a startup achieved by the impingement of compressed air on the turbine rotor to provide an engine speed of 15 to 20 percent prior to ignition.

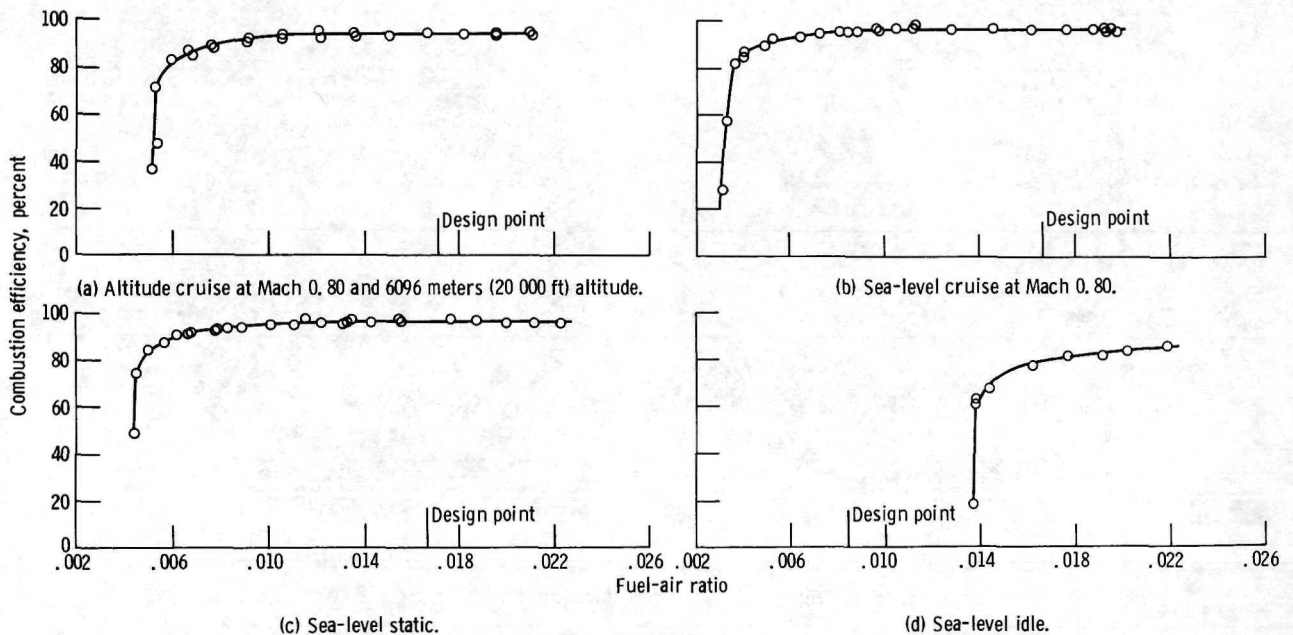


Figure 9. - Effect of fuel-air ratio on combustion efficiency.

The sea-level-idle condition is a test stand condition rather than a mission requirement. However, the results shown in figure 9(d) are of interest in presenting an overall picture of combustor performance because of possible future use of this type of engine for other missions or for aircraft propulsion, where ground operation becomes important. The idle efficiency does not exceed 85 percent even at high fuel-air ratios, and combustion is not maintained at a fuel-air ratio below 0.014. The idle design point for this engine is 50-percent speed, requiring a turbine-inlet temperature of 666 K (740° F). At 100-percent combustion efficiency, the required fuel-air ratio is only 0.0084, a point at which combustion cannot be maintained. If the efficiency data of figure 9(d) are re-plotted as a function of turbine-inlet temperature, as in figure 10, it can be seen that, at the design temperature, a combustion efficiency of approximately 63 percent is achieved. Low efficiency is not unusual for low-temperature, low-pressure idle conditions; however, with present emphasis on control of emissions at airports, this low efficiency might cause a level of unburned hydrocarbons which would be unacceptable. Also, comparison of figures 9(d) and 10 shows that the idle design turbine-inlet temperature is reached at a point where blowout is imminent. Therefore, if the idle performance were to become an important consideration, it would be essential to have an improvement in combustion stability and idle efficiency, or at least an increase in idle speed to reach a higher level of efficiency.

Total-pressure loss. - The combustor isothermal total-pressure loss $\Delta P/P$ is plotted as a function of the diffuser-inlet Mach number in figure 11. At the altitude-cruise design point of Mach 0.8 flight speed at an altitude of 6096 meters (20 000 ft),

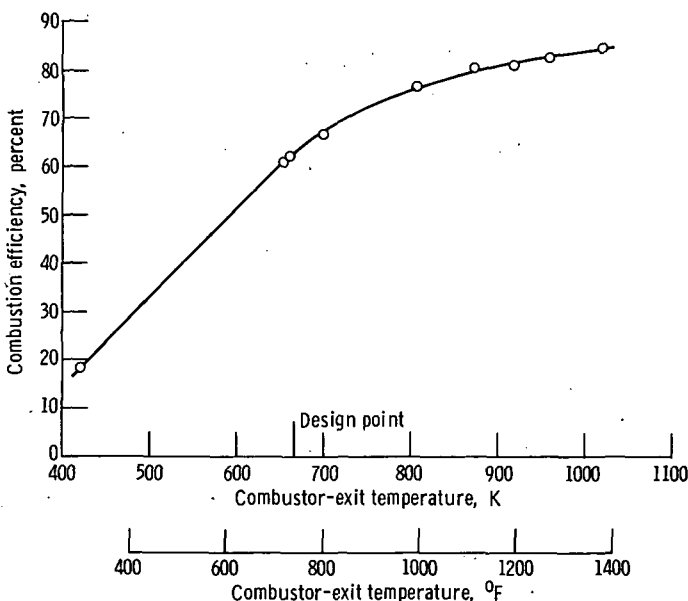


Figure 10. - Effect of combustor-exit temperature on combustion efficiency at sea-level idle.

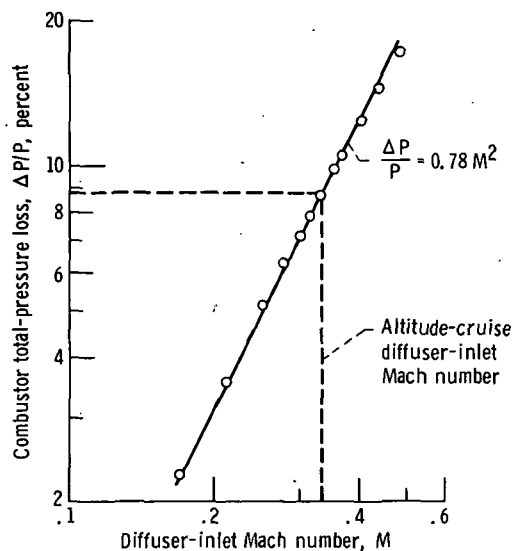


Figure 11. - Variation of combustor isothermal total-pressure loss with diffuser-inlet Mach number. Nominal inlet-air conditions: total pressure, 28.1 N/cm² (40.8 psia); temperature, 291 K (65° F).

the diffuser-inlet Mach number is 0.335, resulting in an isothermal total-pressure loss of approximately 8.8 percent. At the sea-level-cruise design point of Mach 0.8 flight speed, the diffuser-inlet Mach number is 0.355, resulting in an isothermal total-pressure loss of approximately 9.8 percent.

These pressure-loss values are higher than those usually reported for two reasons. The first reason is that the relatively high diffuser-inlet Mach number causes increased diffuser losses. For instance, if a given diffuser has a total-pressure loss of 2 percent at a diffuser-inlet Mach number of 0.25, then at a diffuser-inlet Mach number of 0.35, it will have a loss of nearly 4 percent. This pressure loss contributes nothing to the combustion mixing process and is therefore completely wasted.

The second reason is that the combustor-liner total-pressure losses must necessarily be high because of the high combustor heat-release rate. It has been found that, for high values of heat-release rate, the pressure drop required to achieve sufficient mixing to obtain good combustion efficiency and a good combustor-exit temperature pattern factor is related to the heat-release rate. The relation is shown in figure 12 for a number of current engines. A data point for the combustor of reference 4, from which the test combustor was scaled, is shown for comparison. Figure 12 shows that the heat-release rate has no effect on total-pressure loss until a heat-release rate of approximately 37.3×10^4 joules/hr-cm³-atm (10×10^6 Btu/hr-ft³-atm) is reached. After this point, the total-pressure loss rises steeply with increasing heat-release rate. The altitude-cruise total-pressure loss for the low-cost combustor, including momentum pressure loss, is plotted in figure 12 and follows the trend of the other high-heat-release data.

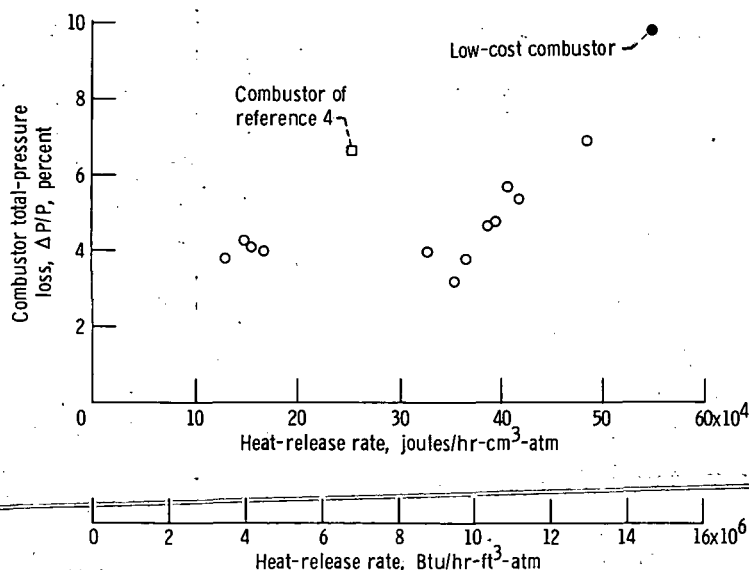


Figure 12. - Relationship of combustor total-pressure loss and heat-release rate for a number of current engines.

Combustor-exit temperature profiles. - In the general case, the required average radial temperature profile at the combustor-exit plane is determined by limitations on the allowable stresses in the turbine rotor blades and the requirements for cooling the combustor-exit transition duct. The maximum allowable temperature is usually located at approximately 70 percent of the distance from the rotor blade hub to the blade tip. In the midspan of the blade, the allowable temperature is limited by the creep strength of the blade material. At the hub, the allowable temperature is limited by the fatigue strength of the blade material. At the tip, the allowable temperature is limited by the high-temperature erosion characteristics of the blade material and the fatigue strength of the stator hub. No study was made to determine a design radial temperature profile for the low-cost engine. The design profile chosen is typical of those used for turbojet engines of similar size and thrust level.

Comparisons of test data with the design average radial temperature profile are presented in figure 13. It must be pointed out that for the short mission times the engine will have, factors such as creep and tip erosion, and possibly even fatigue, lose signifi-

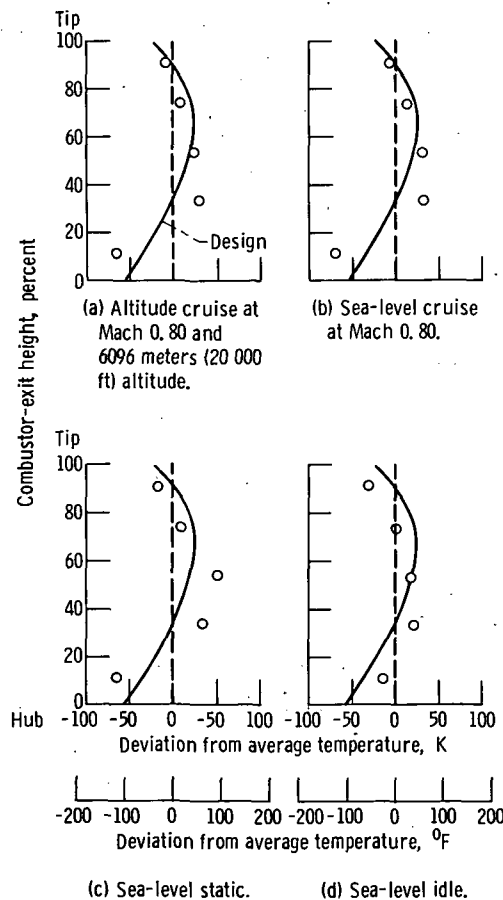


Figure 13. - Combustor average radial exit temperature profile.

cance; therefore, the importance of maintaining the usual "ideal" profile is questionable. In the case under consideration, the turbine stator is made of two rings with the stator blades welded between them, with no provision for expansion. For a favorable stress situation, a uniform radial profile might be desirable, or failing that, a profile hotter at the outside diameter and cooler at the inside diameter to place the stator blades in tension.

The design average circumferential temperature profile at the combustor-exit plane is a uniform one, so that no turbine stator blade has a temperature significantly different from the average. Test results for the design points are shown in figure 14.

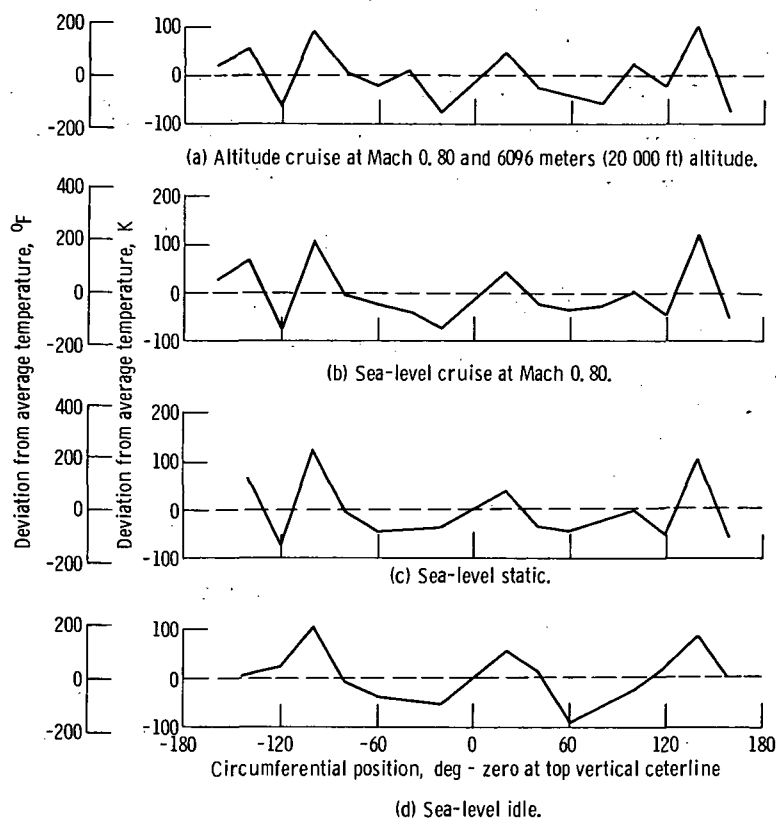


Figure 14. - Combustor average circumferential exit temperature profile.

Three parameters often used to describe the quality of combustor-exit temperature patterns have been defined in the CALCULATIONS section of this report. Values of these parameters, for the same test points for which radial and circumferential profiles have been presented, are given in table IV. Values of the combustor-exit temperature pattern factor $\bar{\delta}$ as a function of the combustor heat-release rate are plotted in figure 15. Figures 15(a) and (b) present data obtained on two separate days for the altitude-cruise and sea-level-cruise conditions, respectively. The repeatability of the data is fairly good, especially at the altitude-cruise condition. It must be kept in mind that even at

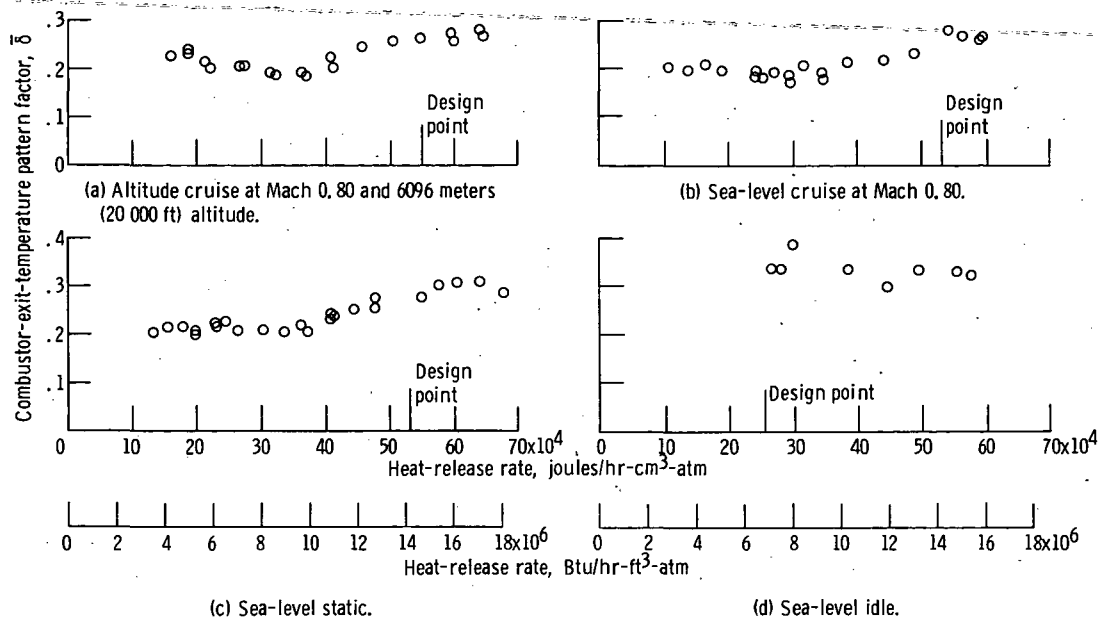


Figure 15. - Effect of heat-release rate on combustor-exit-temperature pattern factor.

the design points, with a combustor temperature rise of approximately 667 K (1200° F), a variation of 0.05 in pattern factor (e.g., from 0.20 to 0.25) is caused by only a 33 K (60° F) variation in the highest individual temperature measured at the combustor exit.

Figure 15(c) presents similar data for the sea-level-static condition, with all data taken during one test session. Figures 15(a), (b), and (c) share a common characteristic in that the pattern factor in all three cases remains at a level near 0.20 until the heat-release rate reaches approximately 37.3×10^4 joules/hr-cm³-atm (10×10^6 Btu/hr-ft³-atm) and then rises gradually to a level near 0.30 as the design heat-release rate is reached.

Figure 15(d) presents similar data for the sea-level-idle condition. The pattern factors shown in this figure are in keeping with the poor idle performance of the combustor, which is caused by the detrimentally low combustor-inlet pressure and temperature at idle.

Ignition and blowout. - Ignition is required at three design points (table V):

- (1) Windmilling at a Mach number of 0.6 at sea level following a rocket-boosted launch
- (2) Static windmilling at sea level with an engine speed of 15 percent of design speed, which is provided by the impingement of compressed air on the turbine rotor
- (3) Windmilling at a Mach number of 0.8 at an altitude of 6096 meters (20 000 ft)

The last point is the altitude-launch design point; however, ignition is desired at any Mach number from 0.5 to 0.8 and at any altitude from sea level to 6096 meters (20 000 ft). Figure 16 shows a map of the altitude windmilling conditions, in terms of

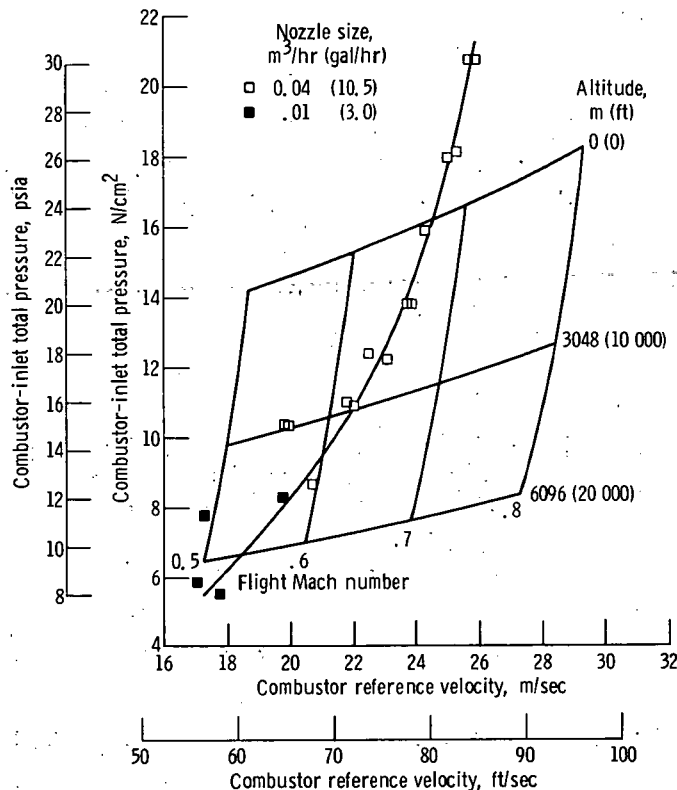


Figure 16. Map of desired windmilling ignition points with combustor blowout limits superimposed.

combustor-inlet total pressure and combustor reference velocity, with combustor test blowout data superimposed. All data are for a fuel-air ratio of 0.020, which is considered to be the maximum value that would not cause excessive combustor-exit temperatures in the test rig. It can be seen that combustion cannot be maintained at the altitude-launch design point, and no method of ignition will succeed unless conditions are altered. In fact, the blowout line obtained with the 0.04-m³/hr (10.5-gal/hr) fuel nozzles does not extend to an altitude of 6096 meters (20 000 ft) even at lower flight Mach numbers.

At the very low engine airflow rates associated with the high-altitude windmilling ignition points, the fuel flow and therefore the fuel nozzle pressure drop are so low that they cause poor fuel atomization. For example, at the design windmilling ignition point of a flight Mach number of 0.8 at an altitude of 6096 meters (20 000 ft), the fuel nozzle pressure drop is 6.1 N/cm² (8.9 psid). A pressure drop of at least 17 N/cm² (25 psid) is required for satisfactory atomization. In order to determine the effect of improved fuel atomization on stable operation at the higher altitudes, the 0.04-m³/hr (10.5-gal/hr) fuel nozzles were replaced with 0.01-m³/hr (3.0-gal/hr) nozzles, with approximately 12 times the pressure drop for equal nozzle flow rates. Figure 16 shows that the im-

proved fuel atomization provided by the $0.01\text{-m}^3/\text{hr}$ (3.0-gal/hr) nozzles allowed stable operation at the windmilling conditions found at altitudes exceeding 6096 meters (20 000 ft), although still at a flight Mach number lower than that desired.

The improvement caused by the higher-pressure-drop nozzles can be seen more clearly in figure 17, where the blowout data shown in figure 16 are replotted, along with ignition data, also at a fuel-air ratio of 0.020. Combustor-inlet total pressure at ignition and at blowout is plotted as a function of airflow rate. As the combustor airflow rate is decreased, both ignition and blowout pressure decrease approximately linearly until an airflow rate of 1.4 kg/sec (3 lbm/sec) is reached. Below this point, ignition is not possible at a fuel-air ratio of 0.020. The blowout data also deteriorate at an airflow rate of 1.1 kg/sec (2.5 lbm/sec). The blowout data shown for lower airflow rates, and for $0.04\text{-m}^3/\text{hr}$ (10.5-gal/hr) fuel nozzles, were obtained by igniting at higher airflow rates and pressures and then lowering the airflow rate to the proper value and obtaining the blowout pressure. The blowout pressures for airflow rates below 1.1 kg/sec (2.5 lbm/sec) depart significantly from the linear relationship found at higher airflow rates. Figure 18 shows that, at an airflow rate of 1.4 kg/sec (3 lbm/sec), the $0.04\text{-m}^3/\text{hr}$ (10.5-gal/hr) nozzle has a pressure drop of 4.5 N/cm^2 (6.6 psid). At the same airflow rate, the $0.01\text{-m}^3/\text{hr}$ (3.0-gal/hr) nozzle has a pressure drop of 55.2 N/cm^2 (80.1 psid). This nozzle also has a pressure drop of 13.8 N/cm^2 (20.0 psid) at the 0.7-kg/sec (1.5-lbm/sec) airflow rate associated with the sea-level air-impingement-start design point.

The improvement in both ignition and blowout with the $0.01\text{-m}^3/\text{hr}$ (3.0-gal/hr) nozzles is evident in figure 17. Both curves were extended linearly to an airflow rate of 0.7 kg/sec (1.5 lbm/sec). The disadvantage of using $0.01\text{-m}^3/\text{hr}$ (3.0-gal/hr) nozzles is that, at the sea-level cruise design point, the required nozzle pressure drop is 787 N/cm^2 (1141 psid), which necessitates a very-high-pressure fuel pump and sturdy manifolding. In order to obtain the advantage of higher nozzle pressure drop at ignition points without the disadvantage of excessive fuel pressure at the flight design points, some form of dual manifolding could be used, so that a lesser number of nozzles could be used during ignition. Since the flow rate of a simplex nozzle is proportional to the square root of the nozzle pressure drop, using half of the nozzles for ignition and thereby doubling the flow per nozzle results in four times as much nozzle pressure drop. Early in the test program, a combustor was tested which differed from the final design in that it had smaller snout air-entry holes and larger liner air-entry holes. Of the 12 nozzle positions, every other one was blanked off in one test; and in another test, eight were blanked off, leaving one nozzle on either side of each igniter. The test condition was the 15-percent-speed air-impingement-start condition, where ignition at a fuel-air ratio of 0.020 was not possible when twelve $0.04\text{-m}^3/\text{hr}$ (10.5-gal/hr) nozzles were used. Figure 19 presents the test data as fuel-air ratio required for ignition as a

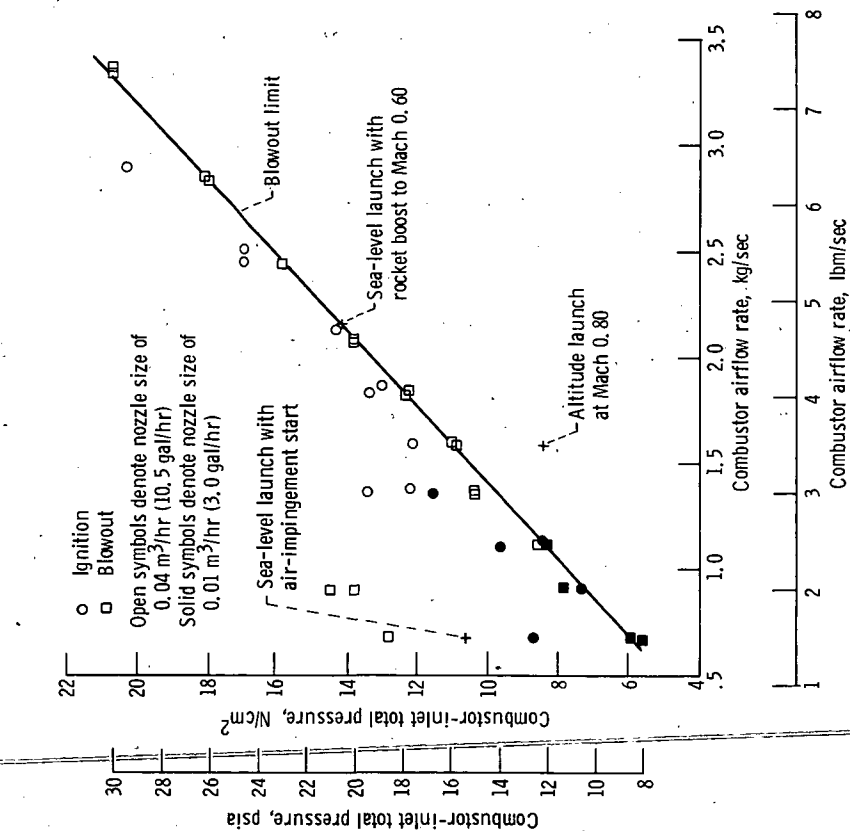


Figure 17. - Combustor ignition and blowout pressure as function of airflow rate. Combustor-inlet total temperature, 311 to 327 K (100° to 130° F); nominal fuel-air ratio, 0.020.

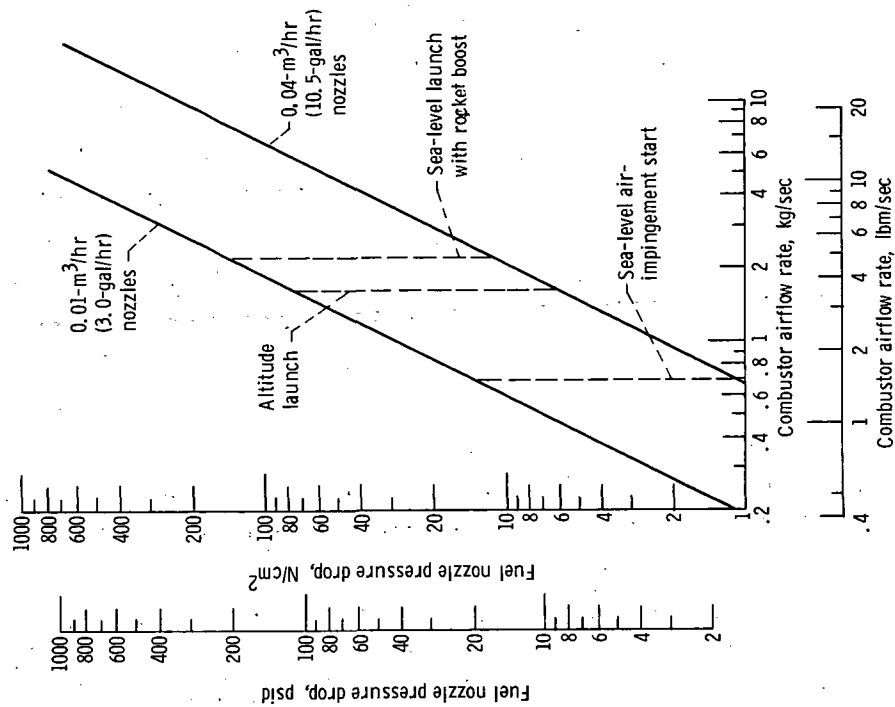


Figure 18. - Fuel nozzle pressure drop as function of combustor airflow rate for constant fuel-air ratio of 0.020.

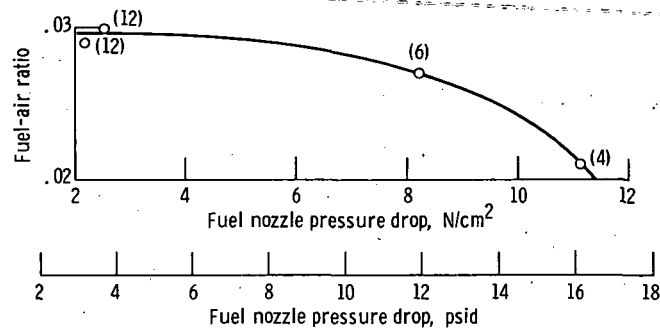


Figure 19. - Effect of fuel nozzle pressure drop on fuel-air ratio required for ignition. Nominal inlet conditions: total pressure, 10.3 N/cm^2 (15.0 psia); temperature, 308 K (95° F). Number of $0.04\text{-m}^3/\text{hr}$ (10.5-gal/hr) nozzles used noted beside each data point.

function of nozzle pressure drop. With only four nozzles and a nozzle pressure drop of 11.2 N/cm^2 (16.2 psid), ignition was obtained at a fuel-air ratio of 0.021, compared with the fuel-air ratio of 0.030 required when all 12 nozzles were used.

Another technique which might be successfully utilized is that of injecting pulses of fuel at high fuel-air ratios so that atomization is improved but the time-averaged fuel-air ratio is not high enough to cause excessive combustor-exit temperatures upon ignition. Also, the allowable fuel-air ratio for ignition might be much higher in the engine than the 0.020 fuel-air ratio to which the combustor test rig is normally limited. The low inertia of the engine allows it to accelerate from windmilling to design speed in only 2 to 4 seconds. Since engine airflow increases immediately upon ignition, the fuel-air ratio could be lowered quickly, and excessive turbine-inlet temperatures could be avoided.

Although these techniques will provide adequate ignition conditions at two of the three ignition design points, the altitude-launch design point poses a more difficult problem. There is a difference of approximately 2.8 N/cm^2 (4 psi) between the combustor-inlet pressure at the design point and the blowout pressure, and an even larger difference at the corresponding ignition pressure. It is doubtful that an increase in the allowable ignition fuel-air ratio will alone overcome these differences. Some means might be used to reduce the airflow rate, thus bringing the altitude-launch ignition point of figure 17 to the left, across the ignition line. Some device will have to be used to keep the engine from windmilling continuously while being carried by the aircraft, in order to avoid bearing failures. A means of reducing airflow at ignition might be incorporated into this device, perhaps a diaphragm on the engine tailpipe that would be designed to blow out upon ignition and acceleration. A combination of reduced airflow rate and increased fuel-air ratio may provide the required ignition conditions.

It should be pointed out that the difficulty of igniting at the altitude windmilling ignition point stems from two sources:

(1) The off-design conditions associated with the altitude windmilling ignition point are very severe.

(2) Development effort was keyed to obtaining a good combustor-exit temperature pattern factor. One of the trade-offs to obtain this was decreased ignition capability.

At the altitude windmilling ignition point, the engine airflow rate is nearly half of that at the altitude-cruise design point, while the compression ratio is very close to 1.0. This causes the diffuser-inlet Mach number to be 0.428 at the altitude windmilling ignition point compared with 0.335 at the altitude-cruise design point, and the isothermal total-pressure loss $\Delta P/P$ to be 0.144 instead of 0.088. The resulting increased mixing in the combustor primary zone is detrimental to ignition because it tends to break up the areas of high local fuel-air ratio necessary for ignition. The increased combustor reference velocity lowers the residence time of the fuel-air mixture in the primary zone, again making ignition more difficult.

One of the design modifications made to improve the combustor-exit temperature pattern factor was an enlargement of the combustor snout air-entry holes to allow more air to enter the primary zone through the fuel-nozzle swirlers. The resulting leaner primary-zone fuel-air ratio and increased mixing made a substantial improvement in the pattern factor, but both factors are detrimental to ignition capability. Some combustor models tested earlier in the development program, with richer primary zones, had somewhat better ignition capability, but their pattern factors were considered to be unacceptable.

It is clear that at the high heat-release rates the combustor experiences, an inter-relationship exists between the combustor-exit temperature pattern factor, total-pressure loss, and ignition capability. For the combustor described in this report, the pattern factor was optimized with some detriment to total-pressure loss and with considerable detriment to ignition capability. Further development work is anticipated to attempt to improve ignition capability without increasing the pattern factor. If engine tests demonstrate that the pattern factor is not a critical parameter and may be allowed to increase, improvements in both ignition capability and total-pressure loss can be achieved.

Emissions. - Measured values of oxides of nitrogen (NO_x), carbon monoxide (CO), unburned hydrocarbons (HC), and smoke number are presented in table VI. Although emissions data are not of direct interest in an ordnance application, they will be of value in the event that this type of engine is considered for civil aircraft applications.

Endurance. - Endurance testing was limited to 15-minute operation at each of the four design points of table I. ~~This time is typical of the mission time expected in an~~ ordnance application. No damage was caused to the combustor during this time.

SUMMARY OF RESULTS

A combustor designed for use in a low-cost engine was tested with ASTM A-1 fuel. The final combustor configuration produced the following results:

1. Combustion efficiency was approximately 94 percent at the altitude-cruise design point and 96 percent at the sea-level-cruise design point.
2. Combustor isothermal total-pressure loss was 8.8 percent at the altitude-cruise-condition diffuser-inlet Mach number of 0.335 and 9.8 percent at the sea-level-cruise-condition diffuser-inlet Mach number of 0.355.
3. Combustor-exit radial temperature profiles were in very good agreement with the design profile at all design conditions, with no experimental radial average temperature differing from the design temperature by more than 33 K (60° F).
4. Combustor-exit circumferential temperature profiles were satisfactory, with only a few experimental circumferential average temperatures differing from the combustor-exit average temperature by more than 50 K (90° F).
5. Combustor-exit temperature pattern quality parameters were good. The pattern factor $\bar{\delta}$ was 0.264 at the altitude-cruise condition, 0.265 at the sea-level-cruise condition, and 0.274 at the sea-level-static condition.
6. Ignition capability must be improved to provide starting at all desired windmilling start points.
7. Exhaust emissions and smoke number are generally low at all test conditions.
8. Endurance testing was limited to approximately 15 minutes at each design condition, a typical mission length for ordnance applications. No damage to the combustor was caused during this time.

Lewis Research Center,
National Aeronautics and Space Administration,
Cleveland, Ohio, May 16, 1973,
501-24.

APPENDIX A

TEST FACILITY

Testing of the combustor described in this report was conducted in a closed-duct test facility in the Engine Research Building of the Lewis Research Center. This facility is illustrated in figure 20.

A heat exchanger, utilizing the exhaust gases of as many as four J-47 combustor cans as a heat source, heated the combustion air to the required combustor-inlet temperatures without vitiation. A large plenum chamber preceding the test section ensured good mixing and temperature uniformity through the use of punched-plate baffles. A bell-mouthed inlet provided a smooth transition to the test section. The hot exhaust gases from the combustor were cooled in a water-spray section before they entered the facility exhaust ducting. Airflow rates and combustor pressures were regulated by remotely controlled valves upstream and downstream of the test section.

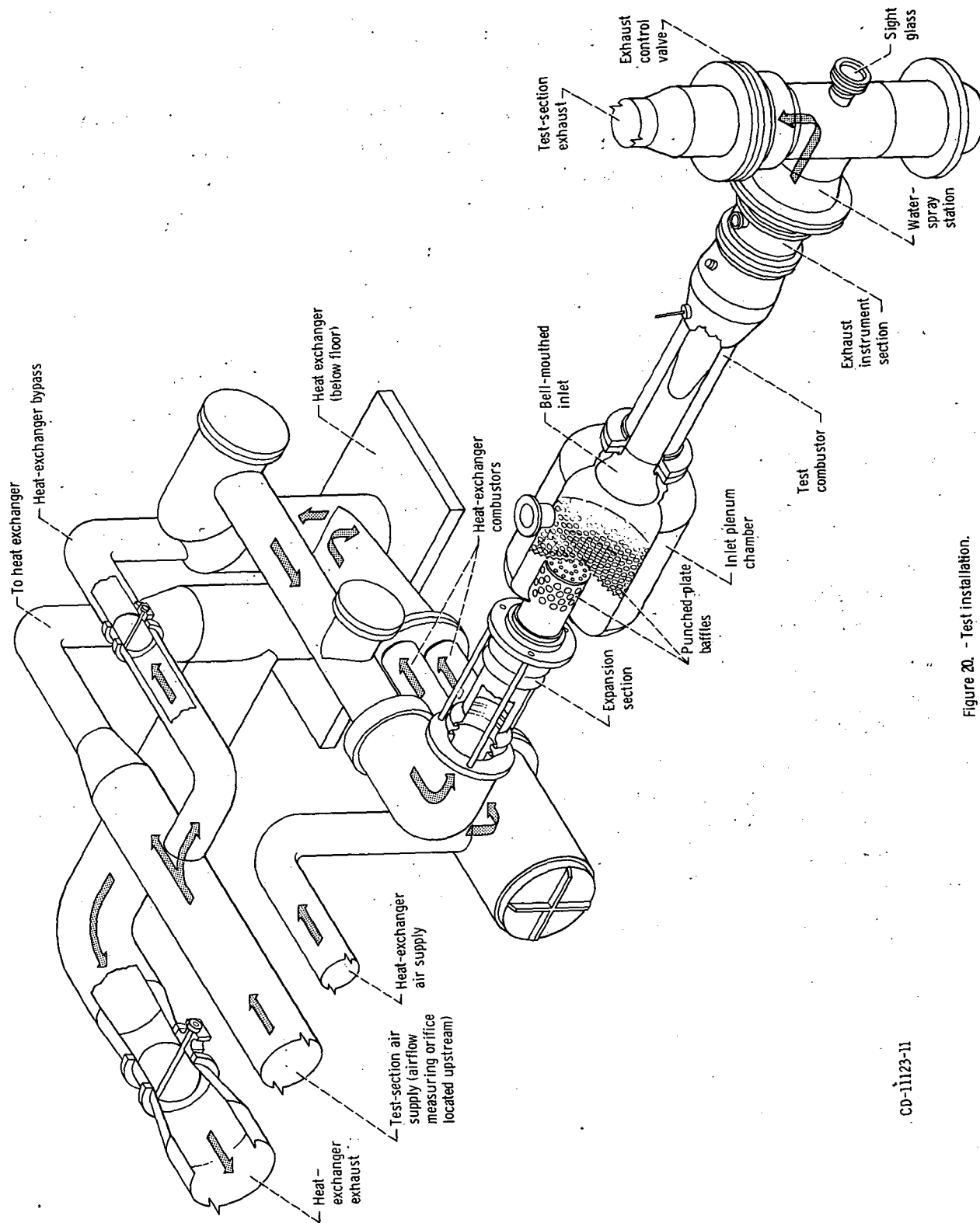


Figure 20. - Test installation.

CD-11123-11

APPENDIX B

INSTRUMENTATION

Test data required to determine combustor performance were recorded at the test facility on punched paper tape. The data were subsequently transferred from the paper tape to a magnetic tape and processed through a digital computer to provide combustor performance results. Control room indicating and recording instrumentation was used to set the test conditions and to monitor the condition of the test section and the test facility. Pressures were measured by strain-gage-type transducers and manometers. Temperatures were measured by iron-constantan and Chromel-Alumel thermocouples of the unshielded wedge type (ref. 13, type 5).

Airflow rates were measured by square-edged orifice plates installed in accordance with ASME specifications. ASTM A-1 fuel-flow rates were measured by turbine flowmeters.

Combustor-inlet total temperature was measured by six equally spaced Chromel-Alumel thermocouples located near the upstream flange of the combustor housing (fig. 21, plane A-A). Inlet-air total pressure was measured by six equally spaced, four-point, total-pressure rakes at the diffuser inlet (fig. 21, plane B-B). At the same location, static pressures at the diffuser inlet were measured by wall static-pressure taps, with six on the outer annulus wall and three on the inner annulus wall.

Combustor-exit total temperature was measured by 16 five-point, Chromel-Alumel, thermocouple rakes spaced as shown in figure 22 and located at the combustor exit (fig. 21, plane C-C). At the same location, combustor-exit total pressure was measured by two five-point total-pressure rakes spaced as shown in figure 22. Static pressure at the combustor exit was measured by wall static-pressure taps, with three on the outer annulus wall and three on the inner annulus wall.

Combustor exhaust emissions and smoke were measured by three equally spaced water-cooled single probes manifolded together and located slightly downstream of the thermocouple rakes (fig. 21, plane D-D).

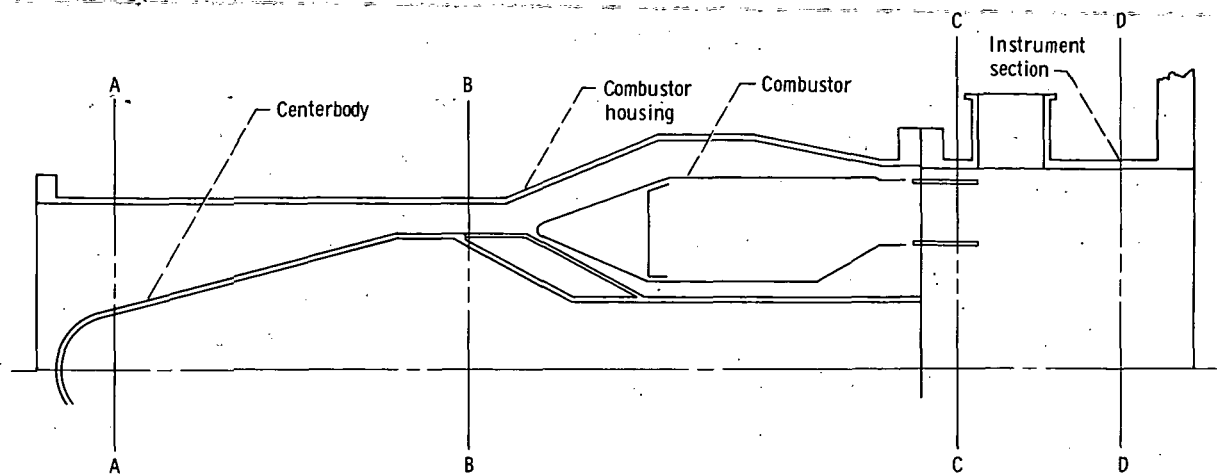


Figure 21. - Schematic drawing of combustor housing and instrument section showing location of instrument planes.

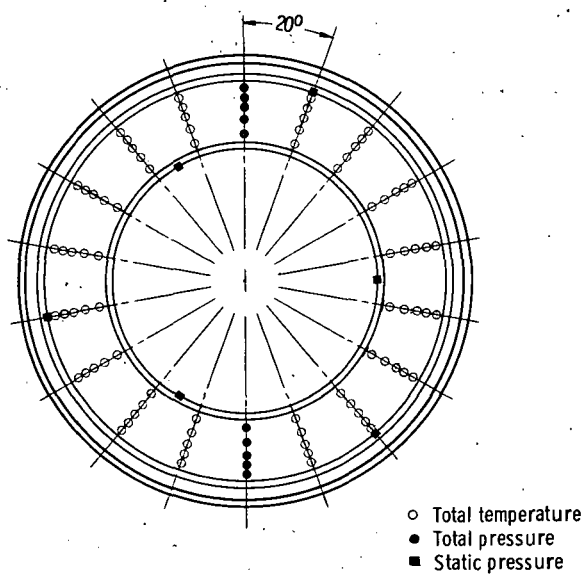


Figure 22. - Combustor-exit instrumentation plane, looking downstream, showing locations of combustor-exit total-temperature probes, combustor-exit total-pressure probes, and combustor-exit static-pressure probes.

REFERENCES

1. Anon.: Aircraft Propulsion. NASA SP-259, 1971.
2. Roelke, Richard J.; and Stewart, Warner L.: Turbojet and Turbofan Cycle Considerations and Engine Configurations for Application in Lightweight Aircraft. NASA TM X-1624, 1968.
3. Dugan, James F., Jr.: Theoretical Performance of Turbojet Engine for Light Subsonic Aircraft. NASA TM X-52538, 1969.
4. Fear, James S.: Performance of a Small Annular Turbojet Combustor Designed for Low Cost. NASA TM X-2476, 1972.
5. Cummings, Robert L.: Experience with Low Cost Jet Engines. NASA TM X-68085, 1972.
6. Norgren, Carl T.: Design and Performance of an Experimental Annular Turbojet Combustor with High-Velocity-Air Admission Through One Wall. NASA Memo 12-28-58E, 1958.
7. Humenik, Francis M.: Performance of a Short-Length Turbojet Combustor Insensitive to Radial Distortion of Inlet Airflow. NASA TN D-5570, 1970.
8. Norgren, Carl T.; and Childs, J. Howard: Effect of Liner Air-Entry Holes, Fuel State, and Combustor Size on Performance of an Annular Turbojet Combustor at Low Pressures and High Air-Flow Rates. NACA RM E52J09, 1953.
9. Goldstein, R. J.; Eckert, E. R. G.; and Ramsey, J. W.: Film Cooling with Injection Through Holes - Adiabatic Wall Temperatures Downstream of a Circular Hole. Paper 68-GT-19, ASME, Mar. 1968.
10. Fear, James S.: Preliminary Evaluation of a Perforated Sheet Film-Cooled Liner in a Turbojet Combustor. NASA TM X-52705, 1969.
11. Anon.: Procedure for the Continuous Sampling and Measurement of Gaseous Emissions from Aircraft Turbine Engines. Aerospace Recommended Practice 1256, SAE, Oct. 1971.
12. Anon.: Aircraft Gas Turbine Engine Exhaust Smoke Measurement. Aerospace Recommended Practice 1179, SAE, May 1970.
13. Glawe, George E.; Simmons, Frederick S.; and Stickney, Truman M.: Radiation and Recovery Corrections and Time Constants of Several Chromel-Alumel Thermocouple Probes in High-Temperature, High-Velocity Gas Streams. NACA TN 3766, 1956.

TABLE I. - NOMINAL COMBUSTOR TEST CONDITIONS

Test point	Design point	Flight altitude		Combustor-inlet total pressure		Combustor-inlet temperature		Airflow rate		Combustor-exit temperature		Reference velocity		Fuel-air ratio required to provide design combustor-exit total temperature at 100-percent combustion efficiency
		m	ft	N/cm ²	psia	K	°F	kg/sec	lbm/sec	K	°F	m/sec	ft/sec	
1	Mach 0.8 cruise	6096	20 000	28.1	40.8	439	331	3.24	7.14	1089	1500	24.5	80.3	0.0171
2	Mach 0.8 cruise	0	0	54.0	78.3	492	426	6.15	13.56	1119	1555	27.1	89.0	.0167
3	Sea-level static	0	0	38.5	55.8	455	359	4.39	9.67	1089	1500	24.8	81.3	.0167
4	Sea-level idle	0	0	13.7	19.9	321	119	1.53	3.38	666	740	17.4	57.0	.0084

TABLE II. - COMBUSTOR DIMENSIONS - FINAL DESIGN

Length, cm (in.):	
Compressor exit to turbine inlet	26.85 (10.570)
Firewall to turbine inlet	16.97 (6.680)
Diameter, cm (in.):	
Inlet, outside	21.03 (8.280)
Inlet, inside	17.37 (6.840)
Exit, outside	24.44 (9.622)
Exit, inside	16.54 (6.510)
Combustor liner volume, m ³ (ft ³)	0.0057 (0.201)
Combustor reference area, cm ² (in. ²)	593.58 (92.00)
Diffuser-inlet area, cm ² (in. ²)	110.3 (17.10)
Open hole area, cm ² (in. ²):	
Snout holes (projected area)	47.68 (7.39)
Swirlers	29.55 (4.58)
Primary-zone hole row	27.16 (4.21)
First diluent hole row	27.16 (4.21)
Second diluent hole row	24.58 (3.81)
Cooling holes in perforated sheet	59.04 (9.15)
Ratio of length to height at reference plane	2.58 (2.58)

TABLE III. - EXPERIMENTAL COMBUSTOR DATA

Test point (see table I) and/or figures where data are used	Run	Combustor-inlet conditions							Combustor operation results									
		Pressure		Temperature		Airflow rate		Reference velocity ft/sec	Diffuser- inlet Mach number	Fuel- air ratio	Exit total temperature		Combustion efficiency, percent	Pressure loss ratio, $\Delta P/P$, percent	Exit temper- ature pattern factor, $\bar{\theta}$	Heat-release rate		
		N/cm ²	psia	K	°F	kg/sec	lbm/sec				K	°F				joules hr-cm ³ -atm	Btu hr-ft ³ -atm	
Test point 1; figures 9(a) and 15(a)	1	27.8	40.3	440	332	3.20	7.05	24.6	80.7	0.345	0.0212	1171	1650	0.938	10.36	0.280	63.7×10 ⁴	17.1×10 ⁶
	2	27.9	40.5	439	331	3.24	7.13	24.7	81.0	.346	.0210	1170	1648	.945	10.10	.268	64.1	17.2
	3	27.9	40.5	439	331	3.24	7.13	24.7	80.9	.345	.0196	1125	1568	.945	9.84	.257	59.6	16.0
	4	27.8	40.3	440	332	3.21	7.06	24.6	80.6	.345	.0196	1122	1562	.939	10.29	.276	59.2	15.9
	5	27.8	40.4	440	332	3.20	7.04	24.4	80.1	.343	.0182	1077	1481	.940	9.94	.264	54.4	14.6
	6	27.8	40.3	439	331	3.20	7.04	24.5	80.2	.343	.0167	1032	1400	.942	9.97	.258	50.3	13.5
	7	27.7	40.2	439	330	3.22	7.09	24.7	80.9	.346	.0151	975	1297	.932	9.95	.246	45.5	12.2
	8	27.8	40.4	439	330	3.21	7.06	24.5	80.2	.343	.0137	927	1211	.929	9.68	.224	40.8	10.9
	9	27.9	40.5	440	333	3.23	7.12	24.7	81.0	.346	.0136	931	1218	.938	9.54	.201	41.0	11.0
	10	27.7	40.2			3.21	7.08	24.7	81.1	.347	.0122	875	1116	.920	9.85	.192	36.1	9.7
	11	28.0	40.6			3.24	7.14	24.7	81.0	.346	.0121	885	1134	.947	9.46	.187	36.9	9.9
	12	27.8	40.4			3.21	7.07	24.6	80.6	.345	.0106	820	1017	.914	9.80	.194	30.9	8.3
	13	28.8	40.6		332	3.24	7.13	24.7	80.9	.345	.0106	829	1034	.939	9.34	.189	32.0	8.6
	14	27.9	40.5		332	3.23	7.11	24.7	80.9	.346	.0092	773	933	.921	9.50	.208	27.2	7.3
	15	27.7	40.2		332	3.21	7.07	24.7	80.9	.346	.0091	764	916	.900	9.80	.204	26.4	7.1
	16	27.8	40.4	438	329	3.18	7.01	24.2	79.5	.341	.0077	703	814	.873	9.40	.215	21.2	5.7
	17	27.9	40.5	438	329	3.23	7.12	24.6	80.6	.344	.0076	710	820	.895	9.10	.203	22.0	5.9
	18	27.7	40.2	439	330	3.20	7.04	24.5	80.2	.344	.0069	670	748	.841	9.46	.231	18.6	5.0
	19	27.8	40.4	437	328	3.24	7.13	24.6	80.7	.346	.0067	671	750	.867	9.18	.237	18.6	5.0
	20	27.8	40.3	439	330	3.23	7.11	24.7	81.0	.346	.0060	640	693	.826	8.93	.225	16.0	4.3
	21	27.6	40.1	439	331	3.19	7.02	24.5	80.4	.345	.0054	543	519	.475	9.24	.698	8.2	2.2
	22	28.1	40.7	439	331	3.21	7.06	24.3	79.7	.340	.0053	593	608	.712	8.81	.266	11.9	3.2
	23	28.4	41.2	438	329	3.22	7.12	24.2	79.3	.337	.0052	515	469	.366	8.39	1.091	6.0	1.6

Test point 2; figures 9(b) and 15(b)	24	53.2	77.1	494	430	6.04	13.31	27.2	89.2	0.364	0.0197	1181	1689	0.956	10.98	0.266	59.2×10 ⁴	15.9×10 ⁶
	25	53.6	77.8	492	427	6.05	13.33	27.0	88.4	.360	.0194	1180	1687	.969	10.64	.259	58.8	15.8
	26	53.4	77.4	493	428	6.03	13.29	27.0	88.6	.365	.0187	1153	1618	.962	11.35	.265	56.2	15.1
	27	53.1	77.0	493	428	6.08	13.40	27.4	89.8	.366	.0176	1120	1559	.962	10.66	.278	54.0	14.5
	28	53.2	77.1	493	428	6.08	13.40	27.4	89.7	.368	.0161	1057	1445	.960	10.82	.229	48.8	13.1
	29	53.5	77.6	492	427	6.08	13.40	27.1	89.0	.362	.0145	1017	1373	.962	10.49	.215	44.0	11.8
	30	53.6	77.7	492	427	6.09	13.31	27.1	89.0	.364	.0127	956	1263	.962	10.70	.211	38.4	10.3
	31	53.4	77.4	492	426	6.09	13.42	27.2	89.3	.365	.0112	914	1187	.982	10.79	.172	34.7	9.3
	32	53.0	76.9	493	428	6.09	13.41	27.5	90.1	.369	.0111	906	1173	.967	10.79	.190	34.3	9.2
	33	53.6	77.7	493	429	6.08	13.39	27.1	88.9	.363	.0104	882	1129	.966	10.36	.205	31.7	8.5
	34	53.4	77.4	494	430	6.09	13.41	27.3	89.6	.367	.0097	856	1083	.961	10.47	.170	29.4	7.9
	35	53.4	77.5	493	429	6.08	13.40	27.2	89.3	.364	.0096	852	1076	.967	10.34	.187	29.1	7.8
	36	53.2	77.2	493	429	6.08	13.40	27.4	89.7	.368	.0088	824	1024	.959	10.51	.195	26.8	7.2
	37	53.6	77.7	494	430	6.09	13.42	27.2	89.3	.364	.0084	806	992	.953	10.40	.180	25.3	6.8
	38	53.4	77.5	493	429	6.08	13.39	27.2	89.3	.363	.0080	792	968	.952	10.58	.193	25.3	6.5
	39	53.5	77.6	493	428	6.15	13.54	27.5	90.0	.369	.0072	760	910	.944	10.46	.183	21.6	5.8
	40	53.6	77.7	493	428	6.12	13.48	27.3	89.6	.366	.0064	730	855	.934	10.39	.195	19.0	5.1
	41	53.3	77.3	492	427	6.10	13.44	27.3	89.6	.367	.0056	699	800	.923	10.41	.207	16.4	4.4
	42	53.5	77.6	493	428	6.07	13.38	27.1	88.9	.363	.0049	668	744	.898	10.18	.195	13.8	3.7
	43	53.1	77.0	493	429	6.07	13.38	27.4	89.7	.367	.0040	629	673	.841	10.31	.202	10.8	2.9
	44	53.6	77.8	491	425	6.11	13.46	27.3	89.4	.372	.0040	630	679	.873	9.79	.260	11.2	3.0
	45	53.3	77.3	↓	↓	↓	13.46	27.5	90.0	.375	.0036	610	639	.821	9.84	.314	9.3	2.5
	46	53.3	77.3	↓	↓	↓	13.47	27.5	90.0	.375	.0032	564	557	.572	9.87	.470	6.0	1.6
	47	53.5	77.6	↓	↓	↓	13.46	27.3	89.6	.372	.0031	527	490	.284	9.40	1.769	3.0	.8

TABLE III. - Continued. EXPERIMENTAL COMBUSTOR DATA

Test point (see table I) and/or figures where data are used	Run	Combustor-inlet conditions							Combustor operation results									
		Pressure		Temperature		Airflow rate		Reference velocity		Diffuser- inlet Mach number	Fuel- air ratio	Exit total temperature		Combust- tion efficiency, percent	Pressure loss ratio, $\Delta P/P$, percent	Exit temper- ature pattern factor, $\bar{\theta}$	Heat-release rate	
		N/cm ²	psia	K	°F	kg/sec	lbm/sec	m/sec	ft/sec			K	°F				joules hr-cm ³ -atm	Btu hr-ft ³ -atm
Test point 3; figures 9(c) and 15(c)	48	38.2	55.4	449	350	4.37	9.63	25.0	81.9	0.346	0.0223	1223	1743	0.952	10.16	0.287	67.4×10 ⁴	18.1×10 ⁶
	49	38.5	55.9	452	354	4.37	9.63	24.8	81.4	.343	.0212	1193	1690	.956	9.83	.310	63.7	17.1
	50	38.5	55.8	453	356	4.36	9.61	24.9	81.6	.344	.0200	1158	1626	.955	9.81	.307	60.4	16.2
	51	38.5	55.8	452	355	4.39	9.66	25.0	82.0	.347	.0188	1117	1567	.963	10.06	.303	57.4	15.4
	52	38.3	55.6	453	357	4.40	9.70	25.3	82.8	.348	.0177	1095	1514	.973	9.94	.275	54.8	14.7
	53	38.1	55.3	453	357	4.39	9.66	25.3	82.8	.350	.0156	1017	1373	.958	10.14	.256	47.7	12.8
	54	38.5	55.9	453	357	4.40	9.69	25.1	82.2	.346	.0155	1024	1386	.972	9.72	.274	47.7	12.8
	55	38.1	55.3	452	355	4.41	9.72	25.4	83.3	.352	.0143	976	1299	.959	9.90	.251	44.3	11.9
	56	38.6	56.0	453	357	4.39	9.67	25.0	82.0	.345	.0135	957	1265	.973	9.48	.234	41.4	11.1
	57	38.5	55.9		357	4.40	9.70	25.1	82.3	.347	.0133	943	1239	.961	9.67	.231	41.2	10.9
	58	38.1	55.2		356	4.47	9.85	25.8	84.7	.359	.0131	934	1223	.958	10.15	.244	41.0	11.0
	59	38.3	55.6		356	4.39	9.68	25.2	82.5	.347	.0122	903	1168	.959	9.65	.206	37.3	10.0
	60	38.6	56.0		357	4.41	9.72	25.1	82.4	.348	.0116	893	1149	.980	9.60	.220	36.1	9.7
	61	38.4	55.7			4.38	9.65	25.1	82.2	.346	.0111	865	1099	.952	9.40	.205	33.5	9.0
	62	38.3	55.5			4.39	9.67	25.2	82.6	.348	.0101	826	1029	.947	9.69	.210	30.2	8.1
63	38.5	55.9			4.39	9.68	25.1	82.2	.346	.0089	784	953	.940	9.36	.206	26.5	7.1	
64	38.3	55.6			4.39	9.68	25.2	82.7	.348	.0083	762	913	.935	9.30	.223	24.6	6.6	
65	38.4	55.7	451	352	4.36	9.60	24.8	81.2	.343	.0079	744	881	.936	9.23	.221	23.1	6.2	
66	38.3	55.6	454	358	4.40	9.69	25.3	82.9	.349	.0078	742	878	.928	9.42	.219	23.1	6.2	
67	38.5	55.8	451	352	4.36	9.61	24.8	81.3	.343	.0068	701	804	.920	9.00	.206	19.8	5.3	
68	38.5	55.8	453	357	4.40	9.69	25.2	82.5	.347	.0067	700	801	.913	9.20	.249	19.8	5.3	
69	38.5	55.8	451	352	4.37	9.62	24.8	81.2	.342	.0062	678	761	.910	9.05	.213	17.9	4.8	
70	38.3	55.6		353	4.34	9.57	24.8	81.2	.342	.0057	651	714	.877	8.88	.215	15.6	4.2	
71	38.4	55.7		353	4.38	9.64	24.9	81.8	.345	.0050	625	666	.849	8.90	.203	13.4	3.6	
72	38.7	56.2		353	4.37	9.63	24.7	81.0	.343	.0045	587	598	.748	8.87	.251	10.4	2.8	
73	38.5	55.8	454	358	4.38	9.64	25.1	82.2	.345	.0044	543	518	.495	9.21	.707	7.1	1.9	

Test point 4; figures 9(d), 10, and 15(d)	74	13.7	19.8	322	121	1.52	3.35	17.4	57.0	0.276	0.0219	1019	1376	0.948	7.17	0.322	57.4x10 ⁴	15.4x10 ⁶
	75	13.7	19.8	322	121	1.52	3.35	17.4	57.2	.277	.0202	959	1289	.830	6.88	.330	55.1	14.8
	76	13.5	19.6	322	120	1.53	3.37	17.6	57.8	.280	.0192	919	1196	.813	7.02	.333	49.2	13.2
	77	13.7	19.8	321	119	1.53	3.36	17.4	57.2	.277	.0177	872	1112	.808	6.69	.298	44.3	11.9
	78	13.7	19.8	322	120	1.51	3.33	17.3	56.8	.274	.0162	806	993	.769	6.58	.335	38.8	10.3
	79	13.6	19.7	321	119	1.52	3.34	17.4	57.2	.277	.0144	699	800	.669	6.70	.389	29.7	8.0
	80	13.2	19.1	↓	↓	1.54	3.39	18.3	59.9	.293	.0138	660	730	.624	7.53	.337	27.9	7.5
	81	13.6	19.7	↓	↓	1.54	3.39	17.7	57.9	.281	.0138	654	719	.612	6.81	.338	26.5	7.1
	82	13.9	20.1	↓	↓	1.53	3.36	17.2	56.3	.272	.0137	421	299	.184	5.78	2.074	7.8	2.1
	83	28.0	40.6	289	61	5.17	11.38	25.9	85.0	0.486	---	---	---	---	17.38	---	---	---
Figure 11	84	28.1	40.7	290	62	4.81	10.60	24.1	79.1	.438	---	---	---	---	14.49	---	---	---
	85	28.1	40.7	290	63	4.52	9.95	22.7	74.3	.403	---	---	---	---	12.41	---	---	---
	86	28.0	40.6	290	63	4.51	9.94	22.7	74.5	.403	---	---	---	---	12.43	---	---	---
	87	28.1	40.7	291	64	4.21	9.27	21.1	69.3	.367	---	---	---	---	10.52	---	---	---
	88	28.1	40.7	289	61	4.12	9.07	20.6	67.5	.357	---	---	---	---	9.88	---	---	---
	89	28.1	40.8	292	66	3.88	8.54	19.5	64.0	.332	---	---	---	---	8.65	---	---	---
	90	28.0	40.6	289	61	3.72	8.19	18.6	61.0	.316	---	---	---	---	7.89	---	---	---
	91	28.2	40.9	292	67	3.59	7.90	18.0	59.0	.302	---	---	---	---	7.17	---	---	---
	92	27.8	40.4	293	68	3.30	7.27	16.8	55.1	.279	---	---	---	---	6.27	---	---	---
	93	28.1	40.7	293	69	3.03	6.67	15.4	50.4	.251	---	---	---	---	5.13	---	---	---
	94	27.9	40.5	294	70	2.57	5.67	13.1	43.0	.211	---	---	---	---	3.55	---	---	---
	95	27.9	40.5	295	71	2.09	4.60	10.7	35.0	.170	---	---	---	---	2.29	---	---	---

TABLE III. - Concluded. EXPERIMENTAL COMBUSTOR DATA

Test point (see table I) and/or figures where data are used	Run	Combustor-inlet conditions										Combustor operation results						
		Pressure		Temperature		Airflow rate		Reference velocity		Diffuser- inlet Mach number	Fuel- air ratio	Exit total temperature		Pressure loss ratio, $\Delta P/P$, percent	Combus- tion efficiency, percent	Exit temper- ature pattern factor, $\bar{\theta}$	Heat-release rate	
		N/cm^2	psia	K	$^{\circ}F$	kg/sec	lbm/sec	m/sec	ft/sec			K	$^{\circ}F$				joules $hr\text{-}cm^3\text{-atm}$	Btu $hr\text{-ft}^3\text{-atm}$
Figures 16 and 17; 0.04-m/hr (10.5-gal/hr) fuel nozzles	96	20.7	30.0	328	131	3.38	7.44	25.9	85.1	---	0.0201	---	---	---	---	---	---	
	97	20.7	30.0	↓	↓	3.37	7.42	25.8	84.8	---	.0200	---	---	---	---	---	---	
	98	20.7	30.0	↓	↓	3.35	7.37	25.7	84.2	---	.0200	---	---	---	---	---	---	
	99	18.1	26.2	↓	↓	2.86	6.29	25.3	83.0	---	.0209	---	---	---	---	---	---	
	100	17.9	26.0	327	130	2.83	6.24	25.1	82.2	---	.0206	---	---	---	---	---	---	
	101	15.9	23.0	327	130	2.44	5.38	24.3	79.8	---	.0204	---	---	---	---	---	---	
	102	13.8	20.0	326	127	2.09	4.61	23.9	78.4	---	.0206	---	---	---	---	---	---	
	103	13.8	20.0	326	128	2.07	4.56	23.7	77.7	---	.0208	---	---	---	---	---	---	
	104	12.2	17.7	315	108	1.85	4.08	23.1	75.8	---	.0197	---	---	---	---	---	---	
	105	12.3	17.9	315	108	1.82	4.01	22.5	73.8	---	.0201	---	---	---	---	---	---	
	106	11.0	16.0	312	103	1.59	3.51	21.8	71.5	---	.0201	---	---	---	---	---	---	
	107	10.9	15.8	102	102	1.59	3.50	22.0	72.1	---	.0200	---	---	---	---	---	---	
	108	10.3	15.0	103	103	1.36	3.00	19.9	65.3	---	.0202	---	---	---	---	---	---	
109	10.3	15.0	103	103	1.36	2.99	19.9	65.2	---	.0201	---	---	---	---	---	---		
110	8.5	12.4	325	126	1.12	2.47	20.6	67.6	---	.0199	---	---	---	---	---	---		
111	14.5	21.0	325	125	.90	1.99	9.8	32.2	---	.0201	---	---	---	---	---	---		
112	13.8	20.0	327	130	.90	1.99	10.4	34.0	---	.0200	---	---	---	---	---	---		
113	12.8	18.6	324	124	.68	1.50	7.9	25.9	---	.0194	---	---	---	---	---	---		

Figures 16 and 17; 0.01-m ³ /hr (3.0-gal/hr) fuel nozzles	114	8.3	12.0	302	84	1.12	2.45	19.7	64.7	----	0.0200	----	----	----	----	----	----	----
	115	7.8	11.3	305	90	.91	2.01	17.3	56.6	----	.0197	----	----	----	----	----	----	----
	116	5.9	8.5	304	87	.68	1.50	17.0	55.8	----	.0195	----	----	----	----	----	----	----
	117	5.5	8.0	307	93	.67	1.47	17.7	58.0	----	.0195	----	----	----	----	----	----	----
Figure 17; 0.04-m ³ /hr (10.5-gal/hr) fuel nozzles	118	23.5	34.1	328	131	3.39	7.46	22.9	75.0	----	0.0202	----	----	----	----	----	----	----
	119	20.3	29.5		↓	2.90	6.38	22.6	74.1	----	.0208	----	----	----	----	----	----	----
	120	17.0	24.6		↓	2.52	5.54	23.6	77.3	----	.0200	----	----	----	----	----	----	----
	121	17.0	24.6		↓	2.45	5.40	22.9	75.2	----	.0200	----	----	----	----	----	----	----
	122	14.3	20.8	326	128	2.13	4.69	23.4	76.9	----	.0208	----	----	----	----	----	----	----
	123	13.0	18.9	317	112	1.87	4.11	22.0	72.2	----	.0200	----	----	----	----	----	----	----
	124	13.4	19.4	313	104	1.83	4.04	20.7	68.0	----	.0201	----	----	----	----	----	----	----
	125	12.1	17.6	313	104	1.59	3.51	19.9	65.2	----	.0201	----	----	----	----	----	----	----
	126	12.2	17.7	313	104	1.38	3.04	17.1	56.2	----	.0199	----	----	----	----	----	----	----
	127	13.4	19.5	312	103	1.37	3.02	15.4	50.5	----	.0199	----	----	----	----	----	----	----
Figure 17; 0.01-m ³ /hr (3.0-gal/hr) fuel nozzles	128	11.6	16.8	300	81	1.36	3.00	17.1	56.2	----	0.0204	----	----	----	----	----	----	----
	129	9.7	14.0	302	84	1.11	2.44	16.8	55.1	----	.0200	----	----	----	----	----	----	----
	130	8.4	12.2	306	91	1.13	2.49	20.0	65.5	----	.0199	----	----	----	----	----	----	----
	131	7.3	10.6	305	89	.91	2.01	18.4	60.4	----	.0198	----	----	----	----	----	----	----
	132	8.8	12.7	306	91	.68	1.49	11.4	37.4	----	.0195	----	----	----	----	----	----	----
Figure 19	133	9.9	14.3	307	94	0.69	1.53	10.4	34.2	----	0.030	----	----	----	----	----	----	----
	134	10.3	15.0	315	108	.67	1.47	9.6	31.5	----	.029	----	----	----	----	----	----	----
	135	10.3	15.0	309	96	.66	1.46	9.6	31.4	----	.027	----	----	----	----	----	----	----
	136	10.5	15.2	307	93	.67	1.48	9.5	31.2	----	.021	----	----	----	----	----	----	----

TABLE IV. - COMBUSTOR-EXIT

TEMPERATURE QUALITY

PARAMETERS

Test point (see table I)	$\bar{\delta}$	δ_{stator}	δ_{rotor}
1	0.264	0.268	0.052
2	.265	.268	-.055
3	.274	.253	.055
4	.337	.343	-.088

TABLE V. - NOMINAL IGNITION POINT COMBUSTOR-INLET CONDITIONS

Design condition.	Altitude		Airflow rate		Pressure		Temperature	
	m	ft	kg/sec	lbm/sec	N/cm ²	psia	K	°F
Altitude launch at Mach 0.8	6096	20 000	1.58	3.49	8.4	12.2	306	91
Sea-level launch with rocket boost to Mach 0.6	0	0	2.15	4.73	14.2	20.6	324	124
Sea-level launch with air- impingement start	0	0	0.68	1.50	10.6	15.4	294	69

TABLE VI. - EXHAUST EMISSIONS DATA

Test point (see table I)	Fuel-air ratio	Exhaust emissions						Smoke number
		Oxides of nitrogen		Carbon monoxide		Hydrocarbons		
		Emissions index, g/kg of fuel	Concen- tration of pollutants, ppm	Emissions index, g/kg of fuel	Concen- tration of pollutants, ppm	Emissions index, g/kg of fuel	Concen- tration of pollutants, ppm	
1	0.0061	1.1	4	155.2	975	49.8	625	2
	.0123	2.1	16	79.5	1000	13.9	350	3
	.0187	2.9	34	53.1	1010	4.0	150	6
2	0.0061	3.9	15	51.7	325	4.0	50	4
	.0119	4.2	31	34.5	420	1.0	25	5
	.0187	4.6	53	24.8	472	.1	4	9
3	0.0063	2.5	10	86.4	560	14.3	185	2
	.0125	3.0	25	50.0	640	3.1	80	4
	.0180	3.7	41	39.0	715	.7	24	9
4	0.0155	0.5	5	-----	-----	54.7	1730	2
	.0201	.8	10	-----	-----	30.0	1225	7

Page intentionally left blank

Page Intentionally Left Blank

NATIONAL AERONAUTICS AND SPACE ADMINISTRATION
WASHINGTON, D.C. 20546

OFFICIAL BUSINESS
PENALTY FOR PRIVATE USE \$300

SPECIAL FOURTH-CLASS RATE
BOOK

POSTAGE AND FEES PAID
NATIONAL AERONAUTICS AND
SPACE ADMINISTRATION
451



POSTMASTER: If Undeliverable (Section 158
Postal Manual) Do Not Return

"The aeronautical and space activities of the United States shall be conducted so as to contribute . . . to the expansion of human knowledge of phenomena in the atmosphere and space. The Administration shall provide for the widest practicable and appropriate dissemination of information concerning its activities and the results thereof."

—NATIONAL AERONAUTICS AND SPACE ACT OF 1958

NASA SCIENTIFIC AND TECHNICAL PUBLICATIONS

TECHNICAL REPORTS: Scientific and technical information considered important, complete, and a lasting contribution to existing knowledge.

TECHNICAL NOTES: Information less broad in scope but nevertheless of importance as a contribution to existing knowledge.

TECHNICAL MEMORANDUMS: Information receiving limited distribution because of preliminary data, security classification, or other reasons. Also includes conference proceedings with either limited or unlimited distribution.

CONTRACTOR REPORTS: Scientific and technical information generated under a NASA contract or grant and considered an important contribution to existing knowledge.

TECHNICAL TRANSLATIONS: Information published in a foreign language considered to merit NASA distribution in English.

SPECIAL PUBLICATIONS: Information derived from or of value to NASA activities. Publications include final reports of major projects, monographs, data compilations, handbooks, sourcebooks, and special bibliographies.

TECHNOLOGY UTILIZATION PUBLICATIONS: Information on technology used by NASA that may be of particular interest in commercial and other non-aerospace applications. Publications include Tech Briefs, Technology Utilization Reports and Technology Surveys.

Details on the availability of these publications may be obtained from:

SCIENTIFIC AND TECHNICAL INFORMATION OFFICE

NATIONAL AERONAUTICS AND SPACE ADMINISTRATION

Washington, D.C. 20546